# Electron self-trapping in liquids and dense gases

John P. Hernandez

*Department of Physics and Astronomy, University of North Carolina, Chapel Hill, North Carolina 27599-3255*

The basic physics regarding self-trapping of light particles in simple fluid hosts is reviewed pedagogically. Electron and positronium self-trapping in fluid helium is taken as a historical starting point. The theoretical context consists of simplified continuum models with averaged interactions, but required improvements are discussed. Experimental examples are chosen to illustrate bulk, surface, and impurity effects. Equilibrium and dynamical aspects of the field are illustrated. In noting applications to more complex systems, reference is made to recent developments using path-integral and computer simulation methods. The article spans certain aspects of studies in this fascinating area over the last 30 years.

## CONTENTS



## I. INTRODUCTION

The subject matter considered in this article focuses on the states available to a light quantum-mechanical particle either in a host whose structure may be locally altered by the interaction with the particle, or in a host that is statically disordered. The possibility that light-particle localization may be highly probable in such systems has important experimental consequences; thus the requirements for such localization are worthy of study. The topic to be addressed can be considered either as an aspect of a broader one dealing with the study of small polarons, particles that are self-consistently accompanied by a local distortion of the host material, or as part of the study of the properties of disordered materials. Therefore the ideas introduced have an applicability beyond the narrower focus discussed. The article treats the basic physics of particle self-trapping in fluid hosts and notes examples of experimental consequences. The theoretical basis is mainly described in terms of a density-functional approach, and recent developments based on path integrals and molecular dynamics are discussed near the end of the article. As an introduction to the topic, the following example gives some motivation.

If one is asked to consider the behavior of an excess electron (from those required for charge neutrality) in an insulating fluid, the first approach that seems suitable is to treat the fluid in some average sense as the source of a potential field in which the electron finds itself and then to deal perturbatively with the intrinsic density fluctuations of the fluid. However, the uncritical application of this philosophy yields results that cannot account for experimental observations of the properties due to excess electrons in a wide spectrum of materials under a variety of experimental conditions. Similar statements are also appropriate regarding other light particles such as the positron or positronium.

As an example, imagine such an approach taken by a naive condensed-matter physicist on being asked, out of the blue, to estimate the drift mobility ($\mu$=drift velocity per unit electric field, in the low-field limit) of excess electrons in liquid helium at 1 atm and 4.2 K. The thoughts of such a physicist might proceed as follows: "What is the low-energy $e$-He interaction? Basically, it is dominated by the repulsive exchange interaction. This dominance results from the Pauli repulsion, the very small polarizability of helium and the instability of $He^-$ (with two electrons in the 1$s$ state of $He^0$). Thus the interaction looks like a hard-sphere repulsion (Jortner *et al.*, 1965) with a radius $a$ that can be estimated from the low-energy $s$-wave scattering length for $e$-He scattering [$a=0.62$ Å for He; had the average interaction been attractive, $a$ would have been negative (O'Malley, 1963)]. Next, how far are the atoms from one another, on average? For the liquid, $\rho=1.88\times10^{22}$ cm$^{-3}$, $\rho^{-1}=4\pi R^3/3$, so $R=2.33$ Å$\equiv3.76a$; thus the volume of the sphere available to an atom is 53 times larger than that of the hard-sphere interaction volume, on average. Therefore the electron is free except for a negligibly small [*sic*] excluded volume." Following this back-of-the-envelope thought, our naive physicist decides that the electron is delocalized in the conduction band and is scattered occasionally. Since the atoms are not really in an ordered array, a quick estimate for the electron mean free path is $(\rho\pi a^2)^{-1}=41$ Å$\approx18R$ and, blithely forging ahead, the mobility can be estimated as the charge-to-mass ratio times the mean scattering time: "$\mu=e\tau/m\approx(e/m)(\rho\pi a^2)^{-1}(m/3kT)^{1/2}=1.6\times10^5$ [cgs]; dividing by 300 to convert to practical units yields $\mu\approx520$ cm$^2$/V s."

An unfortunate experimentalist, armed with this estimate, consults nature. He looks, struggles, checks, and finally returns with his measurement: $\mu\approx2\times10^{-2}$

$cm^2/V\,s$! (Meyer and Reif, 1958.) He faces the theorist, who is not only upset by getting the number wrong but is also faced with incorrect $\rho$ and $T$ dependences, since $\mu$ is found not to be proportional to $\rho^{-1}T^{-1/2}$.

The theorist looks for refinements and argues with himself: "$a$ and $R$ are OK, so what I should do is neglect the atomic motion and assume that the electron is near the bottom of an average conduction band; i.e., using the Wigner-Seitz model (Ashcroft and Mermin, 1976), take a Bloch state for the electron in the band: $\psi(\mathbf{r})=e^{i\mathbf{k}\cdot\mathbf{r}}u_{\mathbf{k}}(\mathbf{r})$ with only a phase shift $e^{i\mathbf{k}\cdot\mathbf{R}'}$ resulting from a displacement by $\mathbf{R}'$ to an equivalent position in another unit cell of an average crystalline model. Then, for the bottom of the band, take $k=0$. Thus, with an atom at the origin,

$$u_0(r<a)=0,\quad u_0(r>a)=(A/r)\sin[k_0(r-a)]\ , \tag{1}$$

with spherical symmetry and a value for $k_0$ to be determined by the boundary condition. To satisfy the average translational symmetry, the derivative of the function $u$ (or better, of its logarithm) must vanish at $R$, the cell boundary. Therefore

$$\tan k_0(R-a)=k_0R\ . \tag{2}$$

The bottom of the band is at

$$E_0=\hbar^2k_0^2/2m\ . \tag{3}$$

Expanding the tangent in a power series yields $E_0$ linear with density at low densities (the so-called optical potential),

$$E_0(\rho\approx 0)\sim\frac{\hbar^2}{2m}4\pi\rho a\ , \tag{4}$$

but it has a stronger density dependence for the case being considered. A numerical solution of the transcendental equation (2), which uses $R$, $a$, and the free-electron mass, yields $E_0=0.98$ eV above the vacuum level. Thus the liquid presents a substantial barrier to the injection of electrons. Stop, look, and note: 0.98 eV is $10^4kT$! Now, backpedal: wouldn't the electron be much happier in a region of lower than average density? After all, the helium atoms are also repelled by the electron!"

Consider the extreme model suggested by the above (Kuper, 1961). Suppose that in the most probable state the electron is localized in a "bubble" of radius $R_0$, devoid of helium inside and with essentially the average helium density outside. In lowest order the electron is confined to the bubble and has a zero-point energy, approximately $\hbar^2\pi^2/2mR_0^2$. The mechanical work that is needed to clear the cavity of atoms is $PV=\frac{4}{3}\pi R_0^3P$; also, a surface (vacuum-liquid helium) has been made at a cost $\sigma A=4\pi R_0^2\sigma$, where $\sigma$ is a surface tension (which we estimate as that of the liquid in equilibrium with its own vapor, with a flat surface—two crude approximations). Proceed to minimize the energy (use $P=1$ atm and the macroscopic $\sigma=0.096$ ergs/cm$^3$) to obtain $R_{0\,\min}=22$ Å. The minimized energy is 0.077 eV for the zero-point energy, 0.028 eV for the $PV$ work, and 0.037 eV for the surface energy. A preferred configuration has been obtained, as this total energy of 0.14 eV is much smaller than that of the electron at the bottom of the average conduction band, the 0.98 eV which was previously estimated. Surely this model is not totally self-consistent, but it is not bad. To put an atom in the cavity would cost an energy of the order of an electron volt, the repulsive potential it would feel due to the electron (which can be crudely approximated by $E_0|\psi|^2\rho$, where $\rho$ is the average density and $|\psi|^2$, obtainable from the particle-in-the-box model, is the average electron probability density over the atomic dimension). Now, with this alternative model for the most probable electron-liquid state, the observed mobility may be estimated as due to a charged sphere of radius $R_0$ moving in a viscous medium (Stokes's law), with kinetic-theory corrections. Stokes's law is

$$\mu=\frac{e}{6\pi\eta R_0}\ , \tag{5}$$

where $\eta$ is the viscosity of the medium (31.7 $\mu$gm/cm s, for liquid He). Using $R_0=22$ Å in this equation yields a mobility of $1.2\times10^{-2}$ $cm^2/V\,s$. This time the result qualitatively agrees with observations to be detailed later, including the temperature and density dependence. Having a short memory, the theorist is no longer upset with himself or the experimentalist!

The lesson to be learned from the above description is that particles, such as electrons, may be trapped in an unstable density fluctuation; once trapped, the particle stabilizes a density inhomogeneity—thus the particle becomes self-trapped. Alternatively, for a static disordered host, although a given local structure may be very improbable in the material, a very small electron energy may be associated with such a structure and, despite the improbability of the local structure, the result is a population of such regions that is strongly favored. This phenomenon is widespread. It is observed in all phases of matter: clusters, solids, liquids, and, as will be shown below, in gases. It occurs in many materials, and the effect also applies to particles other than electrons. This phenomenon falls in the generic class of defects often described as "polarons," although in some cases the interaction may have nothing to do with polarization.

In this review a brief description will be given of "self-trapped" states for electrons, positrons, and positronium in fluids. Emphasis will be placed on a description of the states required to understand experimental observations. As far as materials are concerned, monatomic fluids will be discussed, for simplicity, and only a few comments will be made about more complicated materials, including polar fluids.

## II. SELF-TRAPPING IN LIQUID HELIUM

### A. Bulk effects

Early work on electron self-trapping due to polarization of the medium was begun by Landau (1933). It is

peripheral to this review; so it will not be discussed here. On the other hand, much of the initial impetus to consider the short-range particle-medium interaction was due to electronic phenomena in helium; so we begin with such work (Fetter, 1975; Schwarz, 1975). In the sense of being able to "see" what happens, it is fitting that the original observations and explanations were for positronium (Ps). Ps is the bound electron-positron "atom" which, in vacuum, survives for $10^{-10}$ s in the singlet spin state before annihilation by emission of two gamma rays. In the triplet state, Ps survives for the much longer $10^{-7}$ s, since in that case a three-gamma annihilation is required to conserve angular momentum. In a medium, the long-lived species can decay more rapidly than in vacuum because the positron can always find an electron with opposite spin among those of the host material (pick-off annihilation); naturally, spin conversion processes may also be possible. If the positronium center of mass is delocalized and thus samples the average medium density, the pick-off rate is proportional to the number density in the medium. However, experimental measurements of the decay rate in helium by Paul and Graham (1957), and also by Wackerle and Stump (1957), showed an anomalously slow decay. The observations were immediately explained by Ferrell (1958), who observed that the Pauli-principle repulsion between the electron in Ps and the helium electrons of like spin, in the liquid, would cause a "bubble" to form around Ps and thus decrease the pick-off rate. In the case of Ps interacting with a medium, polarization is negligible, since the Ps atom is neutral. Ferrell assumed that the helium density in the bubble would be that of the coexisting vapor; this assumption was later found to be incorrect.

Observations of electron self-trapping soon were made. Meyer and Reif (1958) measured the electron mobility in liquid helium (below 4 K) and found it to be extremely small. Careri, Scaramuzzi, and Thompson (1959) confirmed the measurements and indeed mentioned the word "bubble" in trying to understand their results. The long-range polarization idea was quickly developed by Atkins (1959) for both positive ions and negatively charged species. He suggested that electrostriction would enhance the density of the material in the neighborhood of charged particles, resulting in the formation of "snowballs." Careri *et al.* (1960) demonstrated the difference between the local environment of positive ions (the snowball) and electrons (the bubble) by extraction experiments across the liquid-vapor surface for $T<2$ K. They could extract electrons with much more ease than positive ions. They quoted Ferrell in order to account for the electron behavior. A detailed "bubble" model for electrons was suggested by Kuper (1961). The theory for electrons in liquid helium became well established and was thoroughly explored in the next few years.

Positronium work lagged behind that for electrons, despite its head start. But it soon provided a startlingly clear verification of the bubbles through measurement of the angular correlation of the two gamma rays emitted in self-annihilation of singlet-Ps in liquid and solid helium (Briscoe, Choi, and Stewart, 1968). As previously noted, the gammas provide for conservation of angular momentum (zero), about the ground-state Ps center of mass, in the annihilation. Naturally, they also conserve the system energy ($2mc^2$) and linear momentum. Conservation of linear momentum was used beautifully to "see" the bubble. The "atom" has a probability distribution of linear momenta, which the coincident gamma rays, from annihilation, faithfully reproduce. The most probable annihilation has antiparallel emission of gamma rays, defining an angle $\theta=0$. The experimental gamma coincidences with one component of linear momentum equal to $mc\theta$ are compared with theory in Fig. 1 ($m$ is the electron mass and $c$ is the speed of light). Annihilations with He-core electrons have been subtracted from the data. The detector geometry consists of long parallel slits and thus integrates over two linear momentum components. Elementary quantum mechanics translates the measured linear momentum distribution of the coincident gammas to $|\psi(r)|^2$ of the Ps center of mass. The particle in a box was beautifully illustrated (Triftshäuser *et al.*, 1968); in the theory, the well depth is obtained from the Wigner-Seitz model and the radius from energy minimization (Hernandez and Choi, 1969), leaving no free parameters. The large angle discrepancy, apparent in the figure, was attributed to incomplete thermalization. More recent positronium work has been reviewed by Iakubov and Khrapak (1982).

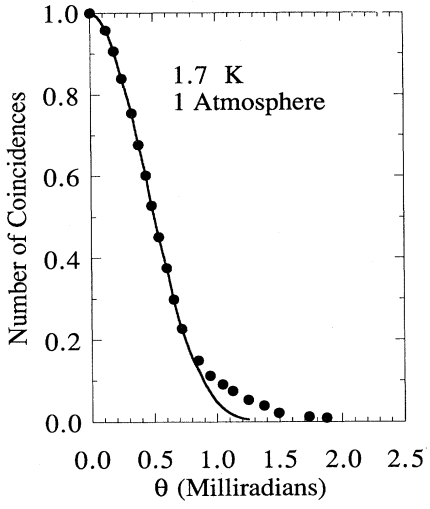


FIG. 1. Two-gamma coincidences, at an angle $\theta$ relative to $\theta=0$ (the collinear case), from annihilation of singlet Ps. The crosses are experimental (Briscoe *et al.*, 1968; Triftshäuser *et al.*, 1968); the line is theoretical for a particle in a well of finite depth and only ground-state occupancy. The discrepancy at large angles was attributed to incomplete thermalization (Hernandez and Choi, 1969).

For probing the properties of electrons in liquid helium, the drift velocity in an applied electric field is the easiest experimental tool to use [in superfluid helium, note the excellent agreement of theory and experiment for both the phonon-limited and roton-limited mobility regimes (Baym *et al.*, 1969)]. Difficulties arise with observations using other experimental techniques, as the electron density that can be studied is limited to very small values ($\sim 10^8$ cm$^{-3}$) due to the electron-electron repulsion and the absence of a compensating positive charge. Nevertheless, clever experimentalists have indirectly probed the electronic optical absorption, using as a basis the argument that photo-ejection of the electron from a bubble should enhance its mobility until retrapping. An ac square-wave electric-field was applied between electrodes in the liquid, with field strength and frequency adjusted to just prevent the drifting bubbles from getting to either of the electrodes. The enhanced mobility on photo-absorption could be demonstrated by applying the light only when the electrons move, say, to the right, and collecting charge. Long integration times can be used to balance small mobility enhancements, and the spectral response can be determined. This is the experiment of Northby and Sanders (1967 and, later, of Zipfel and Sanders, 1968). They observed a photo-ejection threshold corresponding to a well depth of $\sim 1.0$ eV, though the line shape is affected by the vibrational modes of the system. In addition, complications arose due to the surprising fact that bound-bound excitations ($\sim 0.7$ eV, for the $1s$-$2p$ transition) also yielded an enhanced mobility (at $T < T_\lambda$). That phenomenon can be understood as arising from the optically induced release of bubbles from traps. Bubbles bind to vortex lines, regions of quantized mass rotation in the superfluid, by excluding atoms that otherwise would have a rotational kinetic energy (Rayfield and Reif, 1963; Parks and Donnelly, 1966; Springett and Donnelly, 1966; Springett, 1967). On bound optical excitation, thermal energy is released (Jahn-Teller effect) as the environment distorts spontaneously to lift the degeneracy of the excited $p$ state (the populated-state energy is lowered by the distortion). The localized thermal energy generated in this relaxation can release the bubble from its vortex trap; its mobility then increases until retrapping (Fowler and Dexter, 1968; Miyakawa and Dexter, 1970). In the absence of vortices, no such effect is observed for $T > T_\lambda$. Recently, Grimes and Adams (1990) used a technique similar to that described above for detecting the lowest energy absorption by electrons in bubbles ($1s$-$1p$ at $\sim 0.15$ eV for 1.3 K). They note the excellent agreement among various experimental techniques for determining the bubble radii, as a function of pressure and temperature: capture of bubbles by vortices (Springett, 1967), phonon-limited mobility measurements (Ostermeier, 1973), bubble acceleration measurements (Ellis *et al.*, 1983), and their own absorption measurements. Moreover, good agreement is obtained between theory and experiment for the absorption (Miyakawa and Dexter, 1970), and for radii (Padmore and Cole, 1974, if a pressure-independent surface tension is used). Grimes and Adams note that the detailed mechanism for generating the photocurrent they observed, while clearly having to do with release of bubbles from vortices, needs clarification. Finally, there has now been direct observation of the infrared absorption due to electrons in bubbles, obtained by using a long, narrow cell (Grimes, 1991).

### B. Near-surface effects

It is appropriate to mention the topic of electrons on the surface of liquid helium (Cole and Cohen, 1969; Cole, 1970; Shikin, 1970), although it is somewhat peripheral to the discussion in this article (see the early review by Grimes, 1978). A two-dimensional electron gas may be established on the surface of liquid helium. This possibility is due to the large barrier against injection of electrons into the liquid, which was described above, coupled with a weak attraction of external electrons toward the surface. The attraction is a polarization effect that will trap electrons just outside the surface. The trapping potential may be further reinforced by an applied electric field directed perpendicularly outward from the liquid. On charging the surface, the electrons are confined in the perpendicular direction but are still able to move parallel to the surface. As the system is not charge-neutral, a macroscopic potential must be applied to overcome the electron-electron repulsion and prevent total discharge, via a surface current, to the walls of the vessel. It is also possible to trap electron "bubbles," or positive ion "snowballs," just *inside* the helium surface. The polarization effect repels the charged species from the surface and into the bulk (see early work by Bruschi, Maraviglia, and Moss, 1966, for example), but on applying a suitable electric field, attracting the particles toward the surface, a potential minimum is formed, which causes trapping. Pointrenaud and Williams (1972) measured effective masses for such trapped species by monitoring the frequency of their oscillations perpendicular to the surface; coupling to fluid and surface excitation could also be monitored.

Coupling of the external electron plasma to surface excitations was studied at an early stage by Shikin (1971), Sommer and Tanner (1971), and Brown and Grimes (1972). Near-surface charging produces a two-dimensional plasma, which can be probed via the dispersion relation of the plasma waves (see the recent review by Dahm and Vinen, 1987). Grimes and Adams (1976) measured such waves for an electron gas outside the surface. Ott-Rowland *et al.* (1982) looked at plasmons due to interior positive ions, and Barenghi *et al.* (1986) at those due to interior electron bubbles; the damping of the resonances can be used to probe coupled excitations, such as phonons, and quantized capillary waves, ripplons. As the surface electron density can be controlled,

Crandal and Williams (1971) were quick to realize that the competition of the coulomb ($E_c$) versus the thermal energies would lead to solidification of the high-density electron plasma in the classical ($E_c \gg E_F$) regime ($E_F$ is the electron Fermi energy). This suggestion was verified by Grimes and Adams (1979); solidification took place by indentation ("dimpling") of the helium surface accompanying the electron lattice. Fisher *et al.* (1979) provided a more detailed theoretical picture, also noting that quantum melting ($E_F > E_c$) would take place at even higher densities in accord with the two-dimensional model of Kosterlitz and Thouless (1973), which was later developed in work such as that by Nelson and Halperin (1979). Such melting was observed by probing shear waves, in the work of Deville *et al.* (1984). Magnetoplasmons were studied in the electron gas (Mast, Dahm, and Fetter, 1985) and in the electron solid (Glattli *et al.*, 1985).

It was realized that strong dimpling of the surface due to sufficiently strong fields, holding the electrons at the surface, would, at low temperatures, cause trapping of the electrons—a polaron effect that would prevent melting of the solid, as $E_c$ could then become large. The theoretical background for such an effect has been discussed and reviewed by Degani and Hipolito (1985), and the effect may have been observed in mobility studies by Andrei (1984), although the theorists suggest that in the experimental situation there are many electrons per dimple. Situations have been discussed (Leiderer, Ebner, and Shikin, 1982) in which large dimples are formed with $\sim 10^7$ electrons in a dimple; in such cases, for minimization of the Coulombic effects, the surface buckles, and bubbles with such a large total charge are driven into the bulk of the liquid.

Finally, methods for altering electron-ripplon coupling and the ripplon dispersion relation have been devised in which helium films, rather than bulk liquid, underlie the charged arrays. The films are grown on neon, hydrogen, or metallic substrates. Mobility measurements, with film samples, are the subject of work by Kajita and Sasaki (1982) and by Paalanen and Iye (1985); effects of electron scattering by gas atoms, rotons, ripplons, and film defects are observed as well as those due to variations in the film thickness.

As pointed out earlier there is a barrier for injecting electrons into liquid helium, of order 1 eV. But the electrons may reside within bubbles, with an electronic energy of order 50 meV (which depends on pressure and temperature). In addition, there is a barrier for injecting electrons into the vapor, with the barrier height approximately proportional to the vapor density. With this background, the situation can be considered in which electrons reside in bubbles within a liquid that is at coexistence with its own vapor; then, an electric field is applied so the bubbles drift toward the liquid-vapor interface. Under what conditions will it be possible to extract the electrons from the liquid and inject them into the vapor? There is, of course, the question of the mechanism by which particles may be extracted. This depends on the details of the interfacial potential. It was previously noted that charged particles in the liquid would be repelled from the surface due to the polarization effect and that applied electric fields could cause subsurface trapping. Carei *et al.* (1960) were able to extract electrons at low temperatures, but not positive ions. Such results were extended, for example, by Bruschi, Maraviglia, and Moss (1966) and by Schoepe and Rayfield (1973); Cole and Klein (1979) provided theoretical interpretation for the previous paper, and Bruschi *et al.* (1975) carried out experiments of this type in neon. A temperature regime in which the electron extraction is temperature independent was found, indicating that the electrons were no longer being activated thermally and that tunneling through the barrier was taking place. In such cases, the electrons emerge with a kinetic energy $\Delta E = E_{\text{gd(l)}} - E_{\text{0-vap}}$, with the first energy being that of the electron in the bubble ground state within the liquid and the last energy being that of the barrier against electron injection into the vapor at the temperature in question. As the system temperature is raised, the saturated vapor density also rises and eventually coincides with the liquid density at the critical point. Schoepe and Wagner (1975) pointed out that $\Delta E$ would be negative for $T > 4.2$ K and that the tunneling current, observable at low temperatures, would be inhibited. Performing the experiment, they indeed observed an inhibition on raising the temperature. In fact, the inhibition was observed to start at 3.2 K, but there may have been an impurity effect for $3.2 < T < 4.2$ K, which is discussed in a later section. The observed inhibition is a test of the energy contributions, in the two phases, to $\Delta E$.

## III. SELF-TRAPPING IN A FLUID

It might have been expected that self-trapping in helium takes place only in the liquid, but this is not the case. The requirements for electron self-trapping, as the most probable state, are a compromise between a large density of the average medium that makes the delocalized electron energy uncomfortably high, and a compliant medium that allows distortions, needed for electron trapping, without a prohibitive cost in energy. Deviations from the average environment are most prevalent in a fluid; thus a wider spectrum of possible localization environments are available to a light particle in fluid hosts. Since, for helium, the vapor-liquid critical temperature ($T_c$) is 5.20 K and the critical pressure is modest (2.25 atm), experiments can readily be done in the supercritical regime, with the temperature and average density as continuous variables in the gas. Even below $T_c$, electron self-trapping in lower than average density regions has been shown to exist in the vapor at macroscopic fluid densities corresponding to or below that of the saturated vapor, if $T$ is not too low. The alert reader will have noticed that the original argument for localization in a bubble fails for

sufficiently low helium density; in that case, either the smallness of $E_0$ fails to produce bound states, or the binding energy is less than the distortion energy. Indeed, the transition from a high mobility value in the dilute gas to the low mobility at higher fluid density was reported by Levine and Sanders (1962), though full details with an explanatory model were not reported by them until a later paper (1967). Examples obtained later for the mobility transition, as a function of helium number density and temperature, are given in Fig. 2; note evidence of the increased probability of self-trapping on increasing the helium density and lowering the temperature. There is now a report (Borghesani and Santini, 1990b) of similarly compelling data for the mobility transition of electrons in supercritical fluid neon, and related theoretical calculations have been published (Hernandez and Martin, 1991a).

Another example of the transition from a delocalized particle at low fluid density or high temperature to localization on increasing the fluid density or lowering the temperature is the following. In a set of experiments, the mean helium density seen by triplet-Ps in helium was probed. It is reflected by the pick-off rate as a function of the medium density and temperature, as previously noted. At room temperature and helium densities up to $\sim 10^{-2}$ gm cm$^{-3}$, the decay rate $\lambda$ of triplet-Ps is consistent with $\lambda = \lambda_{vac} + b\rho$, where $b$ is a constant, i.e., the vacuum rate plus an average pick-off rate. At lower temperatures and on increasing the helium density, the decay rate turns over and approaches $\lambda_{vac}$ as $T$ decreases and/or $\rho$ increases—a decreased pick-off rate, as the particle-in-an-empty-cavity model becomes appropriate. Measurements are shown in Fig. 3 (Daniel and Stump, 1959; Duff and Heyman, 1962; Roellig and Kelly, 1967; Canter, McNutt, and Roellig, 1975); the solid line is the linear dependence of the room temperature, low-density data. Note that the decay rate shows evidence of localization that takes place more abruptly in density, and at lower densities, for lower temperatures.

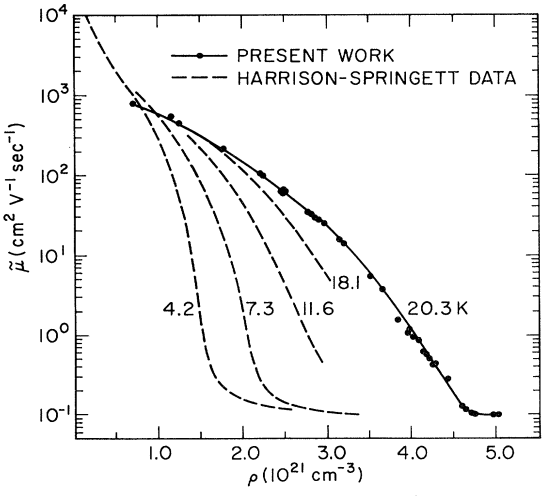


FIG. 2. Effective electron mobility vs helium number density at various temperatures. (The Harrison-Springett data are from 1971a and 1971b. The solid line is data of Jahnke *et al.*, 1975.)

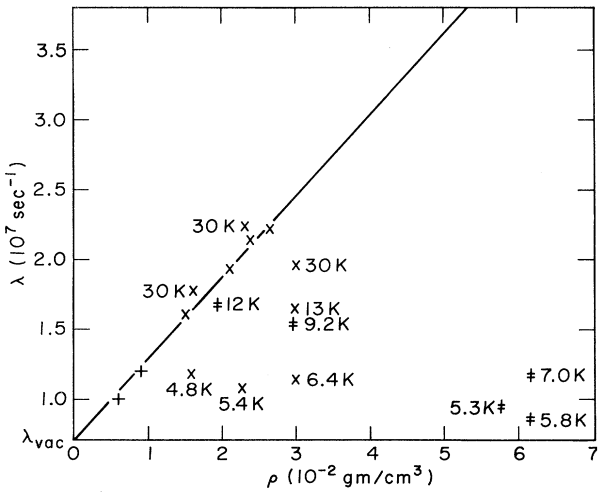


FIG. 3. Triplet-Ps annihilation rate as a function of the mass density of the helium host fluid at various temperatures, as labeled; unlabeled points denote room-temperature data. The measurements are from a variety of experiments (see text). The solid line is characteristic of a delocalized "atom." Note evidence of a localization threshold, with localization taking place more abruptly with density and occurring at lower density for lower temperature (Hernandez, 1976).

To discuss the more general case of self-trapping in the gas, one should be forewarned of a series of complications. In the dense liquid, it was adequate to consider only the most probable state—the empty cavity of a radius $\sim 20$ Å with large potential depth and small ground-state energy in this potential well. As the medium-particle interaction weakens (as is the case with a lower density medium), the most probable state should be expected to have some atoms in the region of low potential for the electron, providing a smoother density profile. Moreover, the distribution of states with nonnegligible probability of occupation, in thermal equilibrium, may not be as well defined as in the dense, low-temperature medium. Such a distribution implies that the observable transition from properties characteristic of the delocalized electron to those of the localized electron need not be sharp. There are conditions in which both localized and delocalized states have appreciable occupation. With these qualitative warnings in mind, discussion now follows of the example that treats the most probable state for a particle interacting via short-range forces with atoms of an ideal gas, at a given temperature. With that example as a basis, the approximations may be reexamined in order to treat a self-interacting fluid, a

more general particle-atom (or molecule) interaction, and to examine the distribution of states. Finally, dynamical questions may, at least, be glanced at.

### A. Ideal gas

Consider a particle of mass $m$, interacting pairwise with much more massive atoms via a contact potential $\gamma\delta(\mathbf{r}-\mathbf{R})$, where $\gamma>0$, $\mathbf{r}$ is the particle coordinate, and $\mathbf{R}$ that of an atomic center. In the average medium, the assumed potential leads to a lowest-energy delocalized state at an energy $E_0=\gamma\rho$, the same result as that obtained previously [Eq. (4)] with a Wigner-Seitz calculation for the low-density fluid. Only one particle is considered, since for a low density of such particles one can ignore interactions among them. Further, the large atomic mass implies that the particle can be considered as interacting with a static atomic distribution; this is the Born-Oppenheimer approximation (1927), which is used throughout the article. In a statistical sense, we shall consider that the atoms constitute a continuum with number density $\rho(\mathbf{R})$ whose average value is $\rho$. In the most probable state of the particle-medium system, we denote the particle wave function as $\psi(\mathbf{r})$ and normalize it. In fact, this is an envelope function, since the details of the particle-atom interaction have been hidden by the contact potential (an average pseudopotential approach). The potential energy felt by the particle is $\gamma\rho(\mathbf{r})$, due to its interaction with the atoms in the medium. Symmetrically, an atom at position $\mathbf{r}$ feels a potential energy $\gamma|\psi(\mathbf{r})|^2$. Since we demand that the atoms be in thermal equilibrium and that they be described as an ideal gas interacting with the particle, their potential energy statistically determines their number density:

$$\rho(\mathbf{r})=\rho\exp(-\gamma|\psi(\mathbf{r})|^2/kT)\ . \tag{6}$$

The equation to be satisfied by the particle is self-consistently determined to be

$$\left[-\frac{\hbar^2}{2m}\nabla^2+\gamma\rho(\mathbf{r})-E\right]\Psi(\mathbf{r})=0\ , \tag{7}$$

with $E$ as the particle eigenvalue. Finally, the system free energy can be written as the particle energy, which includes particle-medium interactions, plus the medium free energy referred to the system with the particle in its lowest-energy delocalized state,

$$\Delta F=(E-\gamma\rho)+\int\rho(\mathbf{r})kT\ln[\rho(\mathbf{r})/\rho]d\mathbf{r} -kT\int[\rho(\mathbf{r})-\rho]d\mathbf{r}\ . \tag{8}$$

In this equation for the free energy, the last two terms are the integrals of $\Delta\mu dN-\Delta P\,dV$, i.e., the chemical potential [$\mu=kT\ln P+\chi(T)$, $P=\rho kT$, with $\chi(T)$ being a function of temperature only] and mechanical energy contributions (other entropy contributions are neglected, for now). The solution of the Schrödinger equation for the particle that minimizes $\Delta F$ is to be sought.

Before examining more general questions, it is instructive to look at the general features of the solution of the illustrative ideal-gas problem that has been posed. Certain limits are easy to solve (Hernandez, 1973). In three

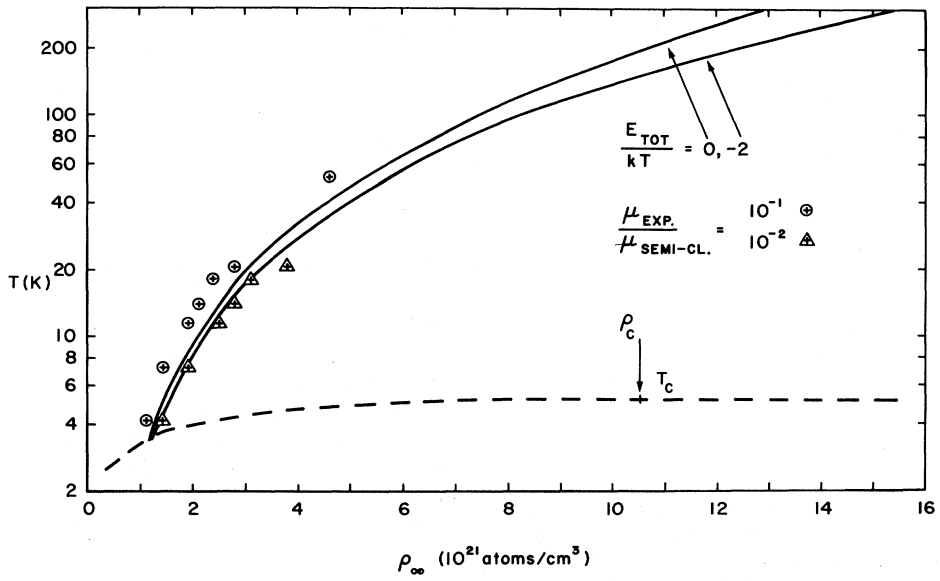


FIG. 4. Locus in density-temperature space of two values of $E_{tot}$ ($\Delta F$ in this article) for electrons in helium, along with points at which the observed mobility is $10^{-1}$ and $10^{-2}$ of that expected, semiclassically, for a delocalized electron in helium; the mobilities are from Levine and Sanders (1967); Harrison and Springett (1971a), (1971b); Jahnke *et al.* (1975). The dashed line is the coexistence line of helium (Hernandez, 1975a).

dimensions, the limits that lead to delocalization as the most probable state are $\rho \to 0$, $\gamma \to 0$, or $T \to \infty$. The self-consistent solution in such cases is $\psi(r) = V^{-1/2}$ (the delocalized state, normalized within a large box of volume $V$, with zero kinetic energy) and $\rho(r) = \rho$, $\Delta F = 0$. A coupling constant, which must be sufficiently large for bound solutions, can be constructed out of ratios comparing a potential versus a kinetic energy for the particle and also potential versus thermal energy contributions (Moore, Cleveland, and Gersch, 1978). Results of calculations yielding values of $\Delta F = 0$ and $-2kT$ are shown in Fig. 4 for helium and can be seen to track the mobility drop of electrons. There is, in fact, also a high $\rho$ limit for binding, due to the atomic size—a physical effect ignored by the ideal-gas model. This new physics leads to a sharply reduced compressibility of the physical system at high density and thus to a positive total energy on localization (Nieminen *et al.*, 1980; Cleveland and Gersch, 1981). Solutions to the nonlinear equation for the ideal-gas case can be obtained directly from computer calculations (Hernandez, 1973, 1975a). Alternatively, a two-parameter analytic approximation can be used, with the parameters fitted to ensure self-consistently at two points and then further improved by perturbation theory (Hernandez, 1975a). A brief discussion of this approach, which is useful to visualize the type of solutions obtained, follows.

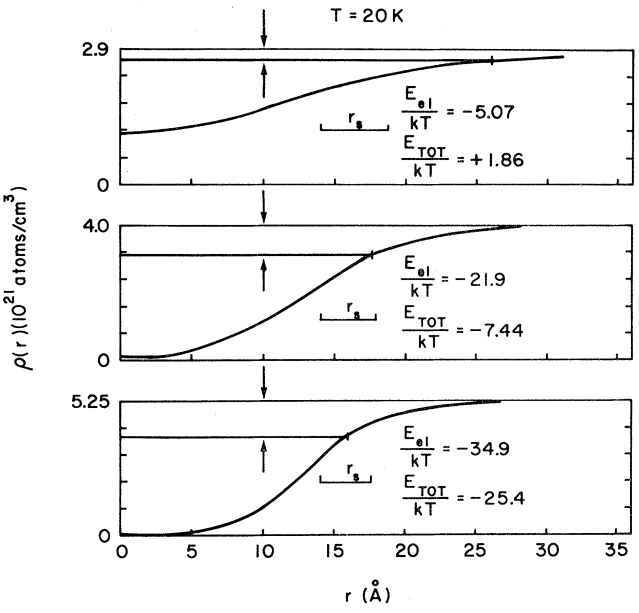


FIG. 5. Density profiles (and also electron potential energy, since it is proportional to the local host density; the arrows denote the electron binding energy) for lowest free-energy electron self-trapped states in helium at 20 K and for the average densities noted. Electron and total free energies (i.e., $\Delta F$) are noted as well as $r_s$, the radius of the mean sphere per atom at the average density. The classical turning point of the electron is noted as the intersection of the horizontal line and the density profile (Hernandez, 1975a).

The method consists of parametrizing the atomic density profile by a function,

$$\frac{\rho(\mathbf{r})}{\rho} = 1 - \frac{C}{\cosh^2 br} , \tag{9}$$

for which the electron Schrödinger equation has known solutions as a function of $C$ and $b$. In this method, $C$ gives the fractional fluid density decrease at the localization center, $r = 0$, and $b^{-1}$ is a radius for the distortion. There is a self-consistent requirement that the chemical potential of the atoms, as a function of their position, when augmented by their interaction with the electron be a constant. This requirement,

$$\ln \frac{\rho(r)}{\rho} = -\frac{\gamma}{kT} |\psi(r)|^2 , \tag{10}$$

allows the parameters $C$ and $b$ to be determined in order to satisfy Eq. (8) at two points ($r = 0$ and $b^{-1}$ are usual). The free energy is then calculated and may be improved with perturbation theory.

The solutions may be visualized, for example, for fixed $m$, $\gamma$, and $T$ as a function of $\rho$. For small $\rho$, the delocalized state has lowest free energy and there is no localized, self-consistent solution. On increasing $\rho$, localized self-consistent solutions are found, but the system state is metastable in comparison with delocalized solutions. Only for large enough $\rho$ is the self-consistent localized solution stable. In such solutions, $C$ increases from $\sim 0.3$ toward unity with increasing bulk $\rho$; so the atoms are increasingly excluded from the localization center. The "radius" ($b^{-1}$) decreases with increasing $\rho$ and the density profile sharpens. At very high $\rho$, the empty-cavity square well is a better starting approximation. See Fig. 5.

To examine nonequilibrium situations and an adiabatic evolution, one may calculate $\Delta F$ for the electron in the ground state of a variety of density profiles, characterized by $b^{-1}$ and $C$, for fixed $m$, $\gamma$, $\rho$, and $T$. The self-consistent constraint (10) is not imposed. At high enough bulk $\rho$ and low $T$, the total-energy contours obtained, as a function of $b^{-1}$ and $C$, will have a minimum (the localized self-consistent solution), a delocalized metastable regime ($C \to 0$, $b$ arbitrary), and a saddle-point configuration connecting the stable and metastable configurations, as a low pass connecting valleys in a mountainous region. With a fixed function for the density profile and a ground-state occupation for the particle, the possible states of the system have not been exhausted, but one will have a reasonable idea of the energy corresponding to various density profiles. See Fig. 6.

### B. Generalizations

Based on the above example, generalizations could be attempted to treat the problem in which the atoms interact with each other (for example, Miller and Reese,

1989 treat a van der Waals fluid) and in which an atom centered at $\mathbf{R}$ interacts with the particle at $\mathbf{r}$ via a more general potential, defined by $v(\mathbf{r}-\mathbf{R})$. In that case the particle potential would be given by $V(\mathbf{r})=\int d\mathbf{R}\, v(\mathbf{r}-\mathbf{R})\rho(\mathbf{R})$. Note that in this continuum model $v(\mathbf{r})$ must be integrable at short range, otherwise a nonvanishing density function leads to a divergent $V(\mathbf{r})$. A $\delta$ function may be used to reflect the short-range electron-atom repulsion, as was done previously, and longer range interactions may be included explicitly. The generalization can be cast as modifications of Eqs. (7) and (8) to

$$\left[-\frac{\hbar^2}{2m}\nabla^2+V(\mathbf{r})-E\right]\psi(\mathbf{r})=0\ , \tag{7'}$$

$$\Delta F=E+\int\{\rho(\mathbf{r})[\mu(\mathbf{r})-\mu]-[P(\mathbf{r})-P]\}d\mathbf{r}\ . \tag{8'}$$

In Eq. (8'), $\mu(r)$ and $P(r)$ refer to the local chemical potential and pressure associated with the density $\rho(r)$, while $\mu$ and $P$ are similarly related to the average fluid density $\rho$. $V(r)$, in Eq. (7'), is a difference between local and average values, so that it vanishes asymptotically. Extremizing (8') with respect to the local-density function implies

$$\left[\rho(r)\frac{\delta\mu(r)}{\delta\rho(r)}-\frac{\delta P(r)}{\delta\rho(r)}\right]+\left[(\mu(r)-\mu)+\frac{\delta V(r)}{\delta\rho(r)}\frac{|\psi(r)|^2}{\langle\psi|\psi\rangle}\right]=0\ . \tag{11}$$

In a local-density approximation the first two terms in Eq. (11) cancel, as required for equilibrium of a "homogeneous" fluid. Then, the requirement that the last two terms in (11) cancel becomes the self-consistent implicit relation between $\rho(r)$ and $\psi(r)$. For example, applying Eq. (11) to the ideal gas yields

$$\left[\rho(r)\frac{\delta(kT\ln[\rho(r)kT])}{\delta\rho(r)}-\frac{\delta(\rho(r)kT)}{\delta\rho(r)}\right]+\left[kT\ln\frac{\rho(r)}{\rho}+\frac{\delta V(r)}{\delta\rho(r)}\frac{|\psi(r)|^2}{\langle\psi|\psi\rangle}\right]=0\ . \tag{11'}$$

The first set of terms indeed vanishes and setting the remaining terms equal to zero yields Eq. (6) for $V(r)=\gamma\rho(r)$. An adiabatic treatment of system excitations can also be attempted, in which the Schrödinger equation is solved and $\Delta F$ determined for arbitrary

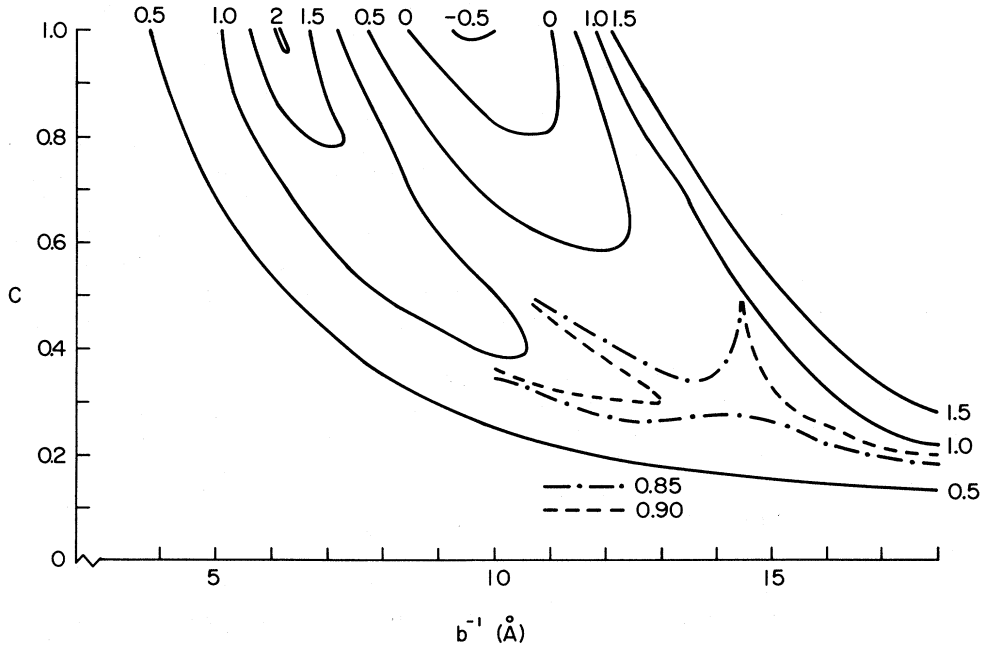


FIG. 6. Total-free-energy contours in units of $kT$ for electrons in helium at 51 K and an average density of $5.5\times10^{21}$ cm$^{-3}$. The axes describe the parametrized helium density profile [Eq. 9, where $C$ is the fractional density decrease at the center of the localization region and $b^{-1}$ is a characteristic radius of the density distortion]. The electron occupies the ground state of the potential associated with the density profile. Note the stable, metastable, and saddle-point configurations, the last being bounded by the dashed and dot-dashed curves (Hernandez, 1975a).

configurations $\rho(\mathbf{R})$. Such an approach may be examined as a guide to population of states other than the most probable one in thermal equilibrium or as a crude guide to the system dynamics, if the adiabatic approximation were considered appropriate as the system evolves toward equilibrium.

Another type of generalization (Martin, 1991; Hernandez and Martin, 1991b) that may be considered consists in inserting the light particle into a fluid, at a temperature below that of its vapor-liquid critical point, and at a density at which it may be expected that the particle will nucleate a local region of the other phase within the average system. For example, an electron in liquid helium may nucleate a bubble; the generalization is then applicable to the problem discussed in the introductory section. The system is defined using Eq. (7′) and (8′), but the latter is generalized by the addition of the term $\sigma \int dA$, where the surface tension $\sigma$ is taken to be curvature independent, for simplicity. Extremizing $\Delta F$ with respect to $\rho(r)$, as before, yields Eq. (11), except in the region in which $\rho_V < \rho(r) < \rho_L$ (the subscripted densities correspond to those of the vapor and liquid at coexistence). A usual approach to the interfacial problem consists of neglecting its detailed structure and assuming that throughout that region $\rho(r)=\rho_V$ or $\rho_L$, with a jump at $r=R$ (the equimolecular dividing surface; see Hirschfelder, Curtiss, and Bird, 1954). As the free energy is a function of a new variable, $\Delta F$ should be extremized with respect to $R$; the functional dependence is contained in $E$, $4\pi\sigma R^2$, and the pressure term with $P(r)$. This last dependence is made explicit by the extremization (at constant $\mu$, $P$, total number of atoms, and volume) as a generalization of the usual procedure:

$$-[P(R^-)-P(R^+)]+[V(R^-)-V(R^+)] \times \frac{|\psi(R)|^2}{\langle\psi|\psi\rangle}+\frac{2\sigma}{R}=0 . \quad (12)$$

The potential terms correspond to those at the coexisting densities of the fluid, with the inner region being the heterophase one; the wave function is continuous at the potential jump. This pressure difference adds a constant pressure term within the new phase region, beyond the dependence of pressure on density from the equation of state; but being a constant, it does not affect Eq. (11). There are now surface terms that contribute to $\Delta F$, beyond those in Eq. (8′), where the surface pressure contributions are not included:

$$\Delta F_S=\frac{4\pi}{3}R^2\left[\sigma+R[V(R^+)-V(R^-)]\frac{|\psi(R)|^2}{\langle\psi|\psi\rangle}\right] . \quad (13)$$

Two thirds of $\sigma A$ has been canceled by part of the surface pressure, the last term in Eq. (12), while a contribution due to the particle surface pressure, which depends on $R$, is now explicit. The definition of $R$ as the equimolecular dividing surface is not adequate to obtain it, since the space dependence of the density is not known in the interfacial region. However, as long as the average system density is not too close to the coexistence curve, all dependences on $R$, and $R$ itself, may be bracketed by the limiting cases defined by the vanishing of (11) at the coexistence densities and the choices $\rho(R)=\rho_V$ or $\rho_L$, implying that the density is $\rho_L$ or $\rho_V$ throughout the interfacial region. The desired results are narrowly bounded by those obtained using these two choices for $R$. The bracket for the results may not be narrow as $\rho$ approaches the coexistence condition, reflecting the model's ignorance of the interfacial region itself. Moreover, as the critical temperature is approached, Eq. (13) tends to zero, due to the vanishing of both $\sigma$ and $\rho_V-\rho_L$. Apparently this formulation, which takes into account the curvature of the surface and the resulting pressure difference, has not been considered previously.

The type of model described in this section suggests that self-trapped bubble states for electrons may be the most probable ones in materials whose gas-phase $s$-wave scattering length is positive: He, Ne, $H_2$, and $N_2$, at sufficiently high $\rho$ and low $T$ (see experimental data by Harrison and Springett, 1971a, 1971b; Bruschi, Mazzi, and Santini, 1972; Loveland *et al.*, 1972; LeComber *et al.*, 1976; Borghesani and Santini, 1990b). Ps will have such states in almost all materials (the short-range repulsion is always dominant). Returning to electrons, in Ar, Kr, and Xe it is no longer reasonable to neglect atomic polarization effects due to the excess electron in comparison with the short-range electron-atom repulsion. Indeed, Ar, Kr, and Xe have negative $s$-wave scattering lengths showing that, in a space-averaged sense, the polarization overwhelms the Pauli repulsion. In fluid Ar there have been suggestions that the effective scattering length changes sign as a function of density (Lekner, 1968a, 1968b), and the experimental mobility studies are most unclear as to localization (Jahnke, Meyer, and Rice, 1971; Huang and Freeman, 1981). For such materials, one should not use a contact potential for the long-range part of the interaction, which should be appropriately screened (Lekner, 1967); and one should consider if self-trapping can arise from enhanced density regions, compared to the average, similar to Atkins's (1959) "snowballs." In these cases the interatomic forces may not be neglected, since the short-range interatomic repulsions are required to prevent the density from growing without bound in the region of electron localization. Such calculations have been performed (Ebner and Punyanitya, 1979; Hernandez, 1983). They delimit density-temperature regions (as in a phase diagram) in which the most probable electron state is predicted to be self-trapped, though no such region was found for argon. Similar calculations have been performed for positrons in helium (Stott and Zaremba, 1977). They resulted in predictions of snowball trapping in regions of the helium phase diagram including the dense vapor, the dilute liquid, and a supercritical region below ~9 K. In the positron case, a direct comparison with experiment is sometimes possible, since the annihilation rate probes the immediate environment of the positron. It is well estab-

lished that there is positron self-trapping in snowballs for helium, methane, argone, hydrogen, nitrogen, $CO_2$, and $SF_6$ (see Iakubov and Khrapak, 1982, who also review positron work, and the recent work by Tuomisaari *et al.*, 1988, who discuss their data in argon and reference work in a variety of other materials).

In contrast to positrons, the experimental situation regarding electron trapping in snowballs is not well established, as electrons are usually probed via mobility studies. These studies may indicate self-trapping by a reduced mobility, but cannot specify the environment of the particle. However, there are several effects, unrelated to self-trapping, that lead to mobility changes associated with delocalized electrons; for example, multiple-scattering effects (O'Malley, 1980; Braglia and Dallacassa, 1982), scattering from fluctuations (Basak and Cohen, 1979), and energy dependence of the scattering cross section (Ramsauer-Townsend effect, for example, or the case of neon: see Borghesani *et al.*, 1988 and Borghesani and Santini, 1990b). The studies in the heavier rare gases, in which snowball trapping might be expected, were reviewed by Holroyd (1987). Measurements along the vapor coexistence line often show decreasing electron mobility on increasing the average fluid density, for some regime. That data could be taken to indicate at least a self-trapping tendency. However, with further density increases (often in the liquid), the mobility increases to a peak that has been correlated with a minimum in the density-dependent average potential felt by electrons in that fluid $[E_0(\rho)]$. The theoretical approximations for the distorted fluid structure for these cases are much less reliable than for those materials in which bubble trapping is predicted (the structure of a dense gas is more difficult to approximate than that of a dilute one). Further discussion will be deferred to a later section.

## IV. ELECTRONS IN A FLUID AS A PROBE

It has been mentioned that electron bubbles in helium below $T_\lambda$ bind to vortices. This binding has been used to observe the position of vortices at the liquid surface and their motion (see Williams and Packard, 1974 and the review by Glaberson and Schwarz, 1987). The observation is accomplished by extraction of the electrons, made to move along the vortex lines to the liquid surface. Upon emerging, the electrons are accelerated to impinge on a phosphorescent screen, which is then photographed.

A more surprising use for electrons in fluids was in molecular spectroscopy. In the only case documented to date, they were used to compare the energies of the $v'=4$ and 5 vibrational states of $O_2^-$ with that of the ground state of $O_2$. Observations of such molecular oxygen impurities in helium were first made and explained by Bartels (1973) at 77 K; there were studies by Jahnke *et al.* (1975) at temperatures from 160 to 52.8 K, and by Bruschi *et al.* (1984a) between 50 and 100 K. (Some data in neon, 77.4 and 293 K, were reported by the last group, 1984b, and they have reported data very recently, 1990a, over a wide density range, at 46.5 K.) For simplicity, imagine the electrons with energy corresponding to the bottom of the average conduction band of the fluid ($E_0$). As a beginning, ignore self-trapping and the energy distribution of the electrons; both effects are of order $kT$ for the modest helium density cases investigated. The energy $E_0$ is above the vacuum level and can be estimated using the Wigner-Seitz model, $\hbar^2 4\pi\rho a/2m$ in the low-density approximation. If such an electron were to be trapped by an $O_2$ molecule, the attachment would initially take place at an energy $E_0 + A$ above the ground state of $O_2^-$ ($A$ is the electron affinity, i.e., the energy difference between the ground state of $O_2$ and that of $O_2^-$; it might be affected by the host fluid, but the effect in the case of helium should be negligible). The probability of such an attachment would be strongly enhanced if there were a resonance between the energy of a vibrationally excited state of the molecular ion and that of the electron. Therefore the vibrational energy levels of the molecular ion can be probed by investigating the attachment rate resonance as a function of $E_0$, i.e., of the helium density. After initial attachment, the molecular ion is stabilized by collision with a third particle, most probably a host atom, which carries away the excess vibrational energy; once molecular vibrational energy has been lost, the electron cannot be easily rereleased from the molecular ion. The attachment is experimentally detected by a reduction of the electron mobility, from its value characteristic within the host to that of $O_2^-$ in the fluid. Figure 7 explains the basis of the phenomenon. The left side of the figure shows the potential of the oxygen molecular ion as a function of internuclear separation. The vibrational states are also shown, and the energy scale is that of $V_0$. The energy zero corresponds to the ground state of the neutral molecule. The top right side shows a plot of the

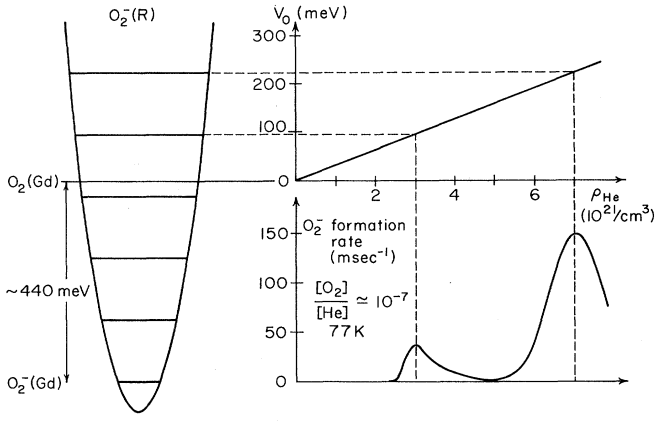


FIG. 7. Resonant electron attachment to molecular oxygen impurity as a function of host, helium, and density. $V_0$ is derived from the Wigner-Seitz model [in this article it is called $E_0$; see Eq. (4)]. The $O_2^-$ formation rate is derived from Bartel's (1973) work. See discussion in the text.

lowest-energy delocalized electron state as a function of the host, helium, and density [in this article it is called $E_0$—see Eq. (4)]. Thus electrons in such states, the initial state when considered along with a ground-state neutral molecule of oxygen, will be in resonance with vibrationally excited molecular ion states, the final states, at helium densities denoted by the dashed lines. Finally, lower right, the formation rate of molecular ions, as deduced from mobility measurements by Bartels (1973), is shown versus helium density. The peaks in the formation rates clearly reflect the electron attachment resonances. Further experimental details are given below.

The experiment proceeds as follows. A pulse of electrons is made to traverse the fluid contained between two electrodes, and the transit time is measured. If there is attachment of some of the electrons to oxygen impurities, the receiving electrode will first record the arrival of the unattached electrons and only later the arrival of $O_2^-$. Since the ratio of the electron mobility to that of $O_2^-$ is at least a factor of 100, the arrival of the $O_2^-$ is readily discriminated from the electron signal, regardless of the place of electron capture within the drift space. The ratio of the number of electrons in the molecular ion group to the total number is a measure of the attachment probability in the electron transit time. This ratio is a function of the helium density, which determines $E_0$. Thus the probability of attachment versus energy is determined by the signal ratio as a function of helium density. To give some feeling for the numbers involved, the average electron mobility at 77 K is $10^2$ ($cm^2V^{-1}s^{-1}$) at a helium density of $3\times10^{21}$ ($cm^{-3}$) and falls to a mobility of about 10 ($cm^2V^{-1}s^{-1}$) at a density of $6\times10^{21}$ ($cm^{-3}$). The $O_2$ concentration in the helium under these conditions was estimated as 0.15 ppm, in the work by Jahnke *et al.*, (1975) and controlled to a fraction of $\sim3\times10^{-8}$, in that of Bruschi *et al.* (1984a). The mobility of $O_2^-$ is $\sim0.1$ ($cm^2V^{-1}s^{-1}$) for these helium densities. In addition, the electron affinity of the molecular ion is known to be 0.44 eV. The states of the molecular ion are in fact doublets, $\Pi_{1/2}$ and $\Pi_{3/2}$. The relevant vibrational energies of $O_2^-$ (above the $O_2$ ground state) are 81 and 101 meV ($v'=4$), and 198 and 216 meV ($v'=5$) (Bartels, 1973). Instead of these doublets, only a single line per vibrational state was detected in all the experiments, although $kT\sim6$ meV. The different vibrational states were, however, well resolved. At the peaks of the resonance attachment, corresponding to helium densities near 3 and 7 ($\times10^{21}$ $cm^{-3}$), there was saturation in that all electrons were captured for a drift space of $\sim1$ cm and a driving field of 100 V/cm in Jahnke's work (see Fig. 8). There is evidence in that work that attachment from self-trapped states is more efficient than from delocalized states, probably due to the immediate stabilization of the molecular ion by the collapsing bubble. Attachment from self-trapped states would imply that the electron energy in such a state, rather than $E_0$, is the relevant variable (see

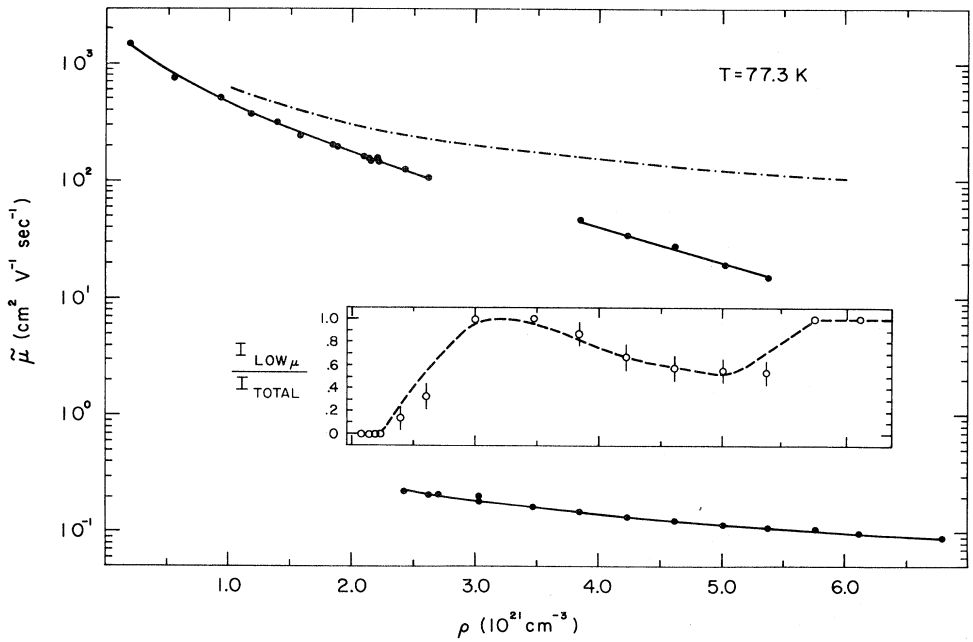


FIG. 8. Apparent mobility vs helium density at 77.3 K. The dot-dashed line is that expected, semiclassically, for delocalized electrons. The upper line is due to unattached electrons, the lower one to $O_2^-$. The insert shows the relative intensity of the low-mobility species. The dashed-line fit is that obtained from Bartels's work (1973) with an assumed $O_2$ concentration of 0.15 ppm (Jahnke *et al.*, 1975).

Hernandez, 1975b; also recall the impurity effect mentioned at the end of the "near-surface" section).

Bruschi *et al.* (1984a) attempted a more detailed analysis of the resonant attachment line shape in order to investigate if it could be used to detect the occupied electron density of states. They had reasonable success using the low-density side of the resonance to obtain a shifted free-particle density of states. However, the high-density side, which would be expected to reflect the density of self-trapped states, was not fit by the semiclassical model they used (that, discussed later in Sec. VI, is due to Eggarter and Cohen, 1970, 1971). The absence of the expected doublet structure in the data is still mysterious and raises questions as to whether the electron density of states is indeed probed directly by the observed line shape. In any case, to within a few millivolts, with a known $E_0(\rho)$—for example, in helium—the vibrational energies of other molecular ions can be studied; alternatively, a known molecular impurity, say $O_2$, can be used to obtain points for $E_0(\rho)$ in other host fluids. The observations in neon (Borghesani and Santini, 1990a) are an example of attempting to use oxygen to probe electron states in that fluid. Resonant attachment is indeed observed to two vibrational states with an energy separation as expected from the variation of the Wigner-Seitz values for $E_0(\rho)$ and the vibrational separation of the molecular ion. However, the neon densities corresponding to the attachment resonances reflect an increase in the electron affinity of oxygen, due to the polarizable host medium (Hernandez and Martin, 1991a). There are still questions to be investigated before this type of probe can be used to full advantage; the method is sensitive to extremely small impurity concentrations and has excellent energy resolution.

## V. REEXAMINATION OF FORMALISM

Up to this point a quite simplified theoretical framework has been used to describe the problem of a light particle in an atomic fluid and to deduce experimentally observable effects in such a system. It is worthwhile to reexamine the methods and approximations that have been introduced in order to describe improvements and to expose more clearly the problems that remain. There are several aspects of the treatment that deserve reexamination. First, there is the fluid itself: a collection of essentially classical particles, at fixed average density and temperature, which interact via a superposition of pair potentials. Then, there is the interaction between the light particle and an isolated atom, the superposition of such interactions corresponding to a collection of atoms at some set of fixed positions, and many-body corrections to such a superposition. Next, there are effects due to atomic motion. Finally, there is the description of the light-particle states and the thermal occupation of the states of the system.

In the description of the fluid itself a thermodynamic approach has been described using a continuum density and an equation of state to relate a local chemical potential, pressure, and fluid density. Such an approach is clearly only consistent with a very slowly varying density profile in an inhomogeneous fluid. A direct approach using the interaction potential among the fluid atoms would bypass the above approximations. Such an approach suggests molecular-dynamics calculations, to be described later.

The particle–isolated-atom interaction has been introduced as parametrized through the low-energy $s$-wave scattering length $a$, an average of the interaction, and a contact potential. Such a description can and should be improved through the use of the energy-dependent electron-atom pseudopotential, an effective interaction that ignores the details internal to the atom but faithfully reproduces the scattering of the electron, due to the atom, in the external region (see, for example, Bachelet *et al.*, 1982; Plenkiewicz, Plenkiewicz, Houée-Levin, and Jay-Gerin, 1988; Plenkiewicz, Plenkiewicz, and Jay-Gerin, 1988). Superposition of such interactions for the particle–many-atom case has merely been taken into account, on average, through the Wigner-Seitz (WS) boundary condition. This feature is also susceptible to improvement. If average properties of the fluid are to be used, the short-range part of the interaction with an atom can be supplemented by long-range features—such as polarization, due to other atoms, using the average pair-correlation function and appropriate screening effects—and then used in the WS cellular model (an early treatment along these lines was that of Springett, Jortner, and Cohen, 1968).

As an aside, the previous description has been used to determine $E_0(\rho)$, within this average approximation, for fluid Kr at various densities by Plenkiewicz, Plenkiewicz, and Jay-Gerin (1989); the results are in reasonable agreement with metal-fluid Kr photoemission measurements (see, for example, Tauchert *et al.*, 1977 and von Zdrojewski *et al.*, 1980). The method described above ignores the inherent disorder in the fluid and thus the generic problem of localization in a statically disordered system (Anderson, 1958). To date there exists no adequate treatment of $E_0(\rho)$ including disorder. Semiclassical attempts have been made to explore a treatment of the problem including disorder (Eggarter and Cohen, 1970, 1971; Eggarter, 1972; Simon *et al.*, 1990). These attempts are based on the semiclassical idea that a particle of sufficiently high energy ($>E_0$) may "percolate" throughout the material (as water may percolate through the interstices of impervious rock grains, if the packing fraction is sufficiently small). Clearly, a quantum particle may tunnel through classically forbidden regions [$E<V(r)$], possibly leading to delocalization, but the phase interference due to scattering in the disordered fluid does lead to localization at sufficiently low energies (Anderson, 1958). The relationship between such a classical percolation threshold and quantum delocalization has not been established.

Throughout the previous discussion the atomic posi-

tions have been kept fixed, at least in some average sense, in contrast to the actual situation in a fluid. The basis for such a treatment is, in principle, the Born-Oppenheimer approximation (1927), a perturbative expansion in terms of a small parameter related to the particle-atom mass ratio. Lowest-order considerations lead to fixed atomic positions. The next-order corrections yield that the particle responds to a potential arising from the instantaneous atomic positions; the particle wave functions are continuously deformed with the changing atomic positions, and the particle energies change adiabatically. It is only in even higher order in the small parameter that the atomic motion causes nonadiabatic transitions of the particle. In equilibrium, such transitions are usually not treated in detail and are replaced by a thermal distribution of particle occupation among its adiabatic states. Alternatively, the time-dependent Schrödinger equation for the light particle may be treated, given the coupled atomic motion. Naturally, the atoms are also coupled to the light particle through an interaction, as well as being coupled to each other. The coupled particle-atomic motions have been examined directly using the adiabatic Born-Oppenheimer approximation; direct propagation of the particle in momentum space is followed by fast Fourier transformation, which allows calculation of the interaction due to the particle acting on the atoms. The process is then repeated. This approach will be discussed later.

The overall description of the light-particle states and thermal occupation of the states of the particle-host system have been discussed in the context of Anderson localized states of a particle in a statically disordered system; the atomic motion is suppressed or thought to be included in the description of the disorder. This approach is discussed in the next section. Alternatively, path-integral techniques have been applied to the thermally averaged motion of the particle coupled to an average or molecular-dynamic treatment of the fluid atoms, as discussed later.

## VI. DISTRIBUTION OF ELECTRON STATES

In order to understand the results of many experiments, it is sufficient to focus on the behavior of particles in the most probable eigenstate of the particle-host system, as far as average occupation is concerned. This is the situation that has been discussed. However, for some experiments such an approach is neither adequate nor reasonable. In some mobility measurements, for example, the most probable eigenstate of the system may not have the ensemble-averaged mobility; in fact, there may be no important eigenstate of the system that has the ensemble-averaged mobility. Some investigators have attempted to circumvent such averaging problems by trying to understand experiments with the idea of a particle with the average properties (leading to concepts such as "quasifree" or "quasilocalized" electrons) or postulating a two-state model (see Young, 1970) in which an electron is sometimes "free" and sometimes "self-trapped"—thus it spends some time in a "fast" state (weakly coupled to the atomic positions) and the remainder in a "slow" (self-trapped) state (see, for example, Huang and Freeman, 1978, regarding experiments in Xe). While it is true that in a system the particles make transitions, it seems more appropriate to recognize that experimental observations, of an ensemble, result from observing an equilibrium or a steady-state distribution over all the states of the system.

The search for the distribution of electron states occupied in thermal equilibrium, as contrasted with focusing only on the most probable state, was first pursued based on a host with a statically disordered set of scatterer positions and a semiclassical treatment of the electron-scatterer interaction (Eggarter and Cohen, 1970, 1971; Eggarter, 1972). In this model, the electron is assumed to sample the scatterer distribution within boxes of side $L$, which are small compared to the sample size. The average potential felt by the electron in such a box is given by the Wigner-Seitz energy [Eq. (3)], with a scatterer density that fluctuates from box to box according to a distribution function characteristic of the material (for example, an ideal gas would have a Gaussian distribution of the number of scatterers per unit volume, with a variance equal to the square root of the average number of scatterers in such a volume). Then, the semiclassical approximation consists in assuming that, within each box, the local electronic density of states is that of a free particle for energies above the local Wigner-Seitz energy. The convolution of the distribution of Wigner-Seitz energies and the local densities of states give an averaged density of electron states, which is then thermally occupied. The model is then extended to predict observed electron mobilities by assuming that there exists an energy-dependent electron mobility, which is to be averaged over the occupied electron states to yield predictions that may be compared with experiment. In this model, electrons are considered able to percolate through the system of boxes if their energy is sufficiently high; then they would have a high mobility. For energies lower than the percolation threshold, given the classically forbidden boxes of high Wigner-Seitz energy, the electrons are localized and have low mobility (allowing atomic motion). The model can be parametrized reasonably to give good fits to experimental measurements. The physical idea of the model is quite appealing, though the semiclassical approximations are a problem.

Alternatively, the distribution of electron states has been pursued using a variational formalism originally due to Luttinger (1976a, 1976b) and suited to disordered systems. The argument proceeds with an electron Hamiltonian

$$H(\mathbf{r},\mathbf{p},\{\mathbf{R}\})=\frac{p^2}{2m}+\sum_{i=1}^{N} v(\mathbf{r}-\mathbf{R}_i)+u_{\text{wall}} , \tag{14}$$

in which the interaction with the atoms, at fixed positions, is given by the sum in the second term, and the last

term ($u_{\text{wall}}$) merely confines the electron to a large but finite volume $V$. The thermodynamic limit, $N, V \to \infty$ with $N/V \to \rho$, will eventually be taken. An ensemble is treated in which the atomic position distribution is given by a probability density $P(\{\mathbf{R}_i\})$, determined by the atomic interactions, the atomic density, and the system temperature. The properties of an ensemble of electrons in a given disordered material are identified with those of electrons in an ensemble of materials with a given $P(\{\mathbf{R}_i\})$. To perform the calculation, the electron partition function, defined by

$$Z(T,\{\mathbf{R}_i\}) = \mathrm{Tr}\{\exp[-H(\mathbf{r},\mathbf{p},\{\mathbf{R}_i\})/k\mathbf{T}]\} , \quad (15)$$

is averaged:

$$\langle Z(T)\rangle = \int P(\{\mathbf{R}_i\}) Z(T,\{\mathbf{R}_i\}) \prod_{i=1}^{N} d\mathbf{R}_i ; \quad (16)$$

the thermodynamic limit is then taken. A variational estimate of $\langle Z(T)\rangle$ is available, as shown below. The electron density of states $\langle g(E)\rangle$ may be obtained by inverse Laplace transforming $\langle Z(T)\rangle$, since

$$\langle Z(T)\rangle = \int_0^\infty \langle g(E)\rangle \exp(-E/kT) dE . \quad (17)$$

A fictional "electron temperature" $T_e$ is used as a variable for the inversion; so one may probe various available energy regions in the spectrum. In contrast, the function $P(\{\mathbf{R}_i\})$ depends on the physical temperature of the system, not on such an electron temperature.

The random example [$P(\{\mathbf{R}_i\}) = V^{-N}$, suitable to describe an ideal gas] is instructive. Luttinger found that in this case

$$\langle Z(T)\rangle \geq \left[\frac{mkT}{2\pi\hbar^2}\right]^{3/2} e^{-C[\chi]/kT} , \quad (18)$$

with

$$C[\chi] = \left\langle \chi \left| \frac{p^2}{2m} \right| \chi \right\rangle + kT \int d\mathbf{r}[\rho - \rho(\mathbf{r})] ,$$
$$\rho(\mathbf{r}) \equiv \rho e^{-\gamma|\chi(\mathbf{r})|^2/kT} , \quad (19)$$

and $(\chi|\chi) = 1$, but $\chi(\mathbf{r})$ otherwise arbitrary. Therefore the lower bound for $\langle Z(T)\rangle$ could be maximized by variation of the functional $C[\chi]$. It may not be a complete surprise that the lower bound is optimized for a normalized $\chi$, which satisfies the equation

$$\left[\frac{p^2}{2m} + \gamma\rho(\mathbf{r}) - E\right]\chi(\mathbf{r}) = 0 , \quad (20)$$

and that the minimized functional is

$$C[\chi]_{\min} = E - \gamma\rho + kT \int d\mathbf{R} \left[\rho - \rho(\mathbf{R}) \left[\ln\frac{\rho(\mathbf{R})}{\rho} - 1\right]\right] . \quad (21)$$

These are the equations obtained previously for the ideal-gas example [Eqs. (6)–(8)], with $\Delta F = C[\chi]_{\min}$. This formulation reemphasizes the interpretation of the optimizing $\chi$, $\rho(\mathbf{r})$, and $\Delta F$ as descriptive of the *most probable* configuration of the particle-host system at a temperature $T$. Although $P(\{\mathbf{R}_i\})$ is uniform, optimization leads to a very particular configuration of scatters $[\rho(r)]$ in the environment of the particle $[\chi(r)]$.

The formalism has been generalized to consider correlations among the atomic positions and several different types of scatterers in order to model interacting fluids and mixtures. For model systems, numerical Laplace inversions have also been carried out to obtain approximations to the average electron density of states $\langle g(E)\rangle$ (Hernandez, 1977; Hernandez, Berger, and Smith, 1979; Berger and Hernandez, 1982; Smith and Hernandez, 1982). The advantage of pursuing this approach is that the density of states allows averaging of the system properties over the *distribution* of thermally occupied states rather than focusing *exclusively* on the most probable state of the system. For example, in gaseous helium at low density, the most probable state is the delocalized electron—but the observed isothermal drift mobility decreases faster than $\rho^{-1}$ (the behavior expected for a delocalized electron; Schwarz, 1980). These observations can be ascribed to the increasing number of localized states as density increases—even though such states are improbable in the low-density gaseous system.

## VII. DYNAMICS OF THERMALIZATION

For completeness, consider the dynamical question of how injected electrons (or, alternately, positrons or Ps) thermalize and self-trap in the case where such states are indeed most probable, once the system achieves thermal equilibrium. This question has not been fully answered, but there does exist experimental information that is yet to be completely understood and assimilated, since it sometimes seems contradictory. The problem to be considered is that of the mechanisms by which an electron, injected with excess kinetic energy into a fluid, achieves thermalization.

It is clear that if the electron is injected with large kinetic energy, energy loss proceeds initially through ionization and excitation of the atomic electrons. Once the energy of the injected particle falls to a level such that it is insufficient to excite the atomic electrons, the only remaining method for energy loss consists in transferring its energy to the motion of the atomic system; the coupling need not be adiabatic. If the system is weakly interacting, one can envision the electron-atom interaction as two-particle elastic scattering. In the case of a more strongly coupled system, energy transfer to collective modes (phonons) is an appropriate description.

In the example of positrons ($e^+$) injected with an energy of 0.5 MeV (from the decay of $Na^{22}$) into saturated helium vapor at $T = 4$ K ($kT = 0.34$ meV), the number of annihilations as a function of time after injection can be followed, since injection is accompanied by a 1.28 MeV gamma ray from the daughter nucleus. This is the case

in which the interaction ($e^+$-He) is the long-range polarization that results in self-trapping in snowballs. The experiments (Tawel and Canter, 1986) and Monte Carlo simulations (Farazdel, 1986) agree, with thermalization proceeding via elastic scattering (after the positron kinetic energy falls first below 19.8 eV, the lowest excitation energy of He, and then below 17.7 eV, the difference between the ionization energies of He and Ps). These slow positions, which are only elastically scattered, appear to be localized below the mobility edge of the disordered material, i.e., below the energy separating extended and localized states, when they reach a kinetic energy of $(E_c^+) \sim 15$ meV, at about 26 ns after injection. They then self-trap on reaching a kinetic energy of $\sim 5$ meV ($E_R$), after about 32 ns, by binding to a cluster of atoms. It is presumed that such an atomic cluster arises due to intrinsic density fluctuations. The experimental signal for localization is the inability of the positron to respond appreciably to an applied electric field (in contrast to the response in a delocalized state). The annihilation rate is assumed constant for energies down to $E_R$, whether localized or not. Self-trapping by binding to a nucleating cluster is signaled by an enhanced pick-off annihilation rate. The kinetic energy, referred to above, is measured from the average potential in the system. There is no problem with this procedure in the (classical, except for quantum-mechanical cross sections) Monte Carlo simulations, but, since the potential fluctuates, the kinetic energy is not well defined in the quantum system. Clearly, the localization energy refers to a total energy, positron plus fluid. Time and positron energy become correlated in this system due to a deep minimum in the energy-dependent-scattering cross section, at positron energy of about 1 eV, which monoenergizes the positrons.

In contrast to the above picture are the results of measurements for electrons injected into helium, among other materials, using a tunnel diode with a gold surface in contact with the fluid (Onn and Silver, 1969, 1971; Smejtec *et al.*, 1973). The electrons are injected with an excess kinetic energy of order 1 eV. After injection, they "see" an image potential attracting them back to the gold electrode and an applied electric field aiding injection. The sum of these two potential contributions has a maximum whose position, relative to the gold electrode, may be varied by adjusting the strength of the applied field. An electron that backscatters into the gold or thermalizes on the gold side of the potential maximum has negligible probability of being collected far from the electrode. Thus a distance scale for thermalization is established in the experiment. The backscattering is determined from measurement of the maximum available current (injection into vacuum) and of the actual current collected through the medium, in the limit of large applied field. The collected current as a function of field (i.e., as a function of the position of the potential maximum), after corrections for backscattering, allows calculation of the fraction of electrons that thermalized beyond the potential maximum. The distance scale can be converted into an estimate for the thermalization time using the average speed of electrons before thermalization.

For injection into argon, where the self-trapping of electrons remains to be clearly demonstrated, the experimental results for the thermalization time are consistent with the elastic-scattering model; *but this is not the case for helium.* The difference seems to reside in the electron-medium interaction, even beyond differences in the elastic-scattering cross sections (Nakanishi and Schrader, 1986a, 1986b). For helium, the short-range repulsion is clearly dominant and results in self-trapping within bubbles. In the experiments described above, for liquid helium at 4.2 K and 1 atm, the electrons appear to thermalize in a time of $\sim 2 \times 10^{-13}$ s, instead of the approximately $10^{-10}$ s predicted by the two-particle elastic-collision model. The range of densities and temperatures covered in these experiments was large: it encompassed the liquid and vapor regimes. Furthermore, variation of the injection energy by a factor of 2 did not affect the thermalization time by large factors. Moreover, the measurements indicate that the thermalization time varies with the reciprocal of the fluid density; this dependence is consistent with the two-particle elastic-collision model as the rate-limiting step. If all the collisions were indeed simply two-particle elastic ones, the electrons could have lost at most only 10 percent of their initial kinetic energy in the thermalization time observed experimentally. Thus it is concluded that inelastic collisions are required and that the thermalization process is more complicated in this case.

These experiments suggest that the electrons find, rather than cause, a suitable localization region in the fluid and then proceed to thermalize into that region very efficiently. The conclusion that the initial localization region is found, not caused, is not unexpected, since the medium has, intrinsically, a broad density-fluctuation spectrum in thermal equilibrium and the electron cannot aid substantially in establishing the trapping potential unless it is already localized. But that the electrons should thermalize efficiently into such regions is quite surprising. There appears to be no reason to believe that electrons are substantially localized, and therefore strongly coupled, in the attractive region upon initially finding it, since at that time they have a very large kinetic energy compared to $kT$. Hence how is it that electrons lose their energy to the distortion, in order to localize rapidly? Might it be that the attractive potential wells met by the electron have resonant states in the continuum and that in such states the electron *does* have a localized component that leads to strong, local coupling with the distortion via the short-range interaction? Such a speculation might be investigated in order to try to develop an explanation for the observed differences in the dynamical localization time: the long time is characteristic of elastic two-particle scattering, for systems with a long-range interaction, and a much shorter time is observed for systems in which the particle-medium interaction is predominantly short ranged.

## VIII. MORE COMPLEX SYSTEMS AND TECHNIQUES

The problem of a light particle interacting with a relatively simple material composed of spherically symmetric atoms has been discussed. The case of fluid $H_2$ or $N_2$ can be treated by the same methods by considering the small molecule in an averaged sense. A natural progression would be to turn to more complicated materials such as He-Ne mixtures, to fluids of larger nonpolar molecules such as ethane, to polar fluids such as water or ammonia, and to molten salts; finite clusters of atoms with an excess electron are also of interest. Indeed, some work along the lines previously discussed exists in all these areas, with a substantial amount for metal-ammonia solutions (as discussed by Kestner, 1976, who also reviews the hydrated electron). In the case where alkali metals are dissolved in ammonia, each metal atom dissociated to yield a cation and an electron: thus the overall system is neutral, allowing for substantial concentrations of electrons. In dilute solutions, the properties due to the electrons in the medium are independent of the choice of cation; the study of such systems has a history of over a hundred years, beginning with Weyl's observation (1863) of the characteristic blue color due to the "solvated" (i.e., self-trapped) electrons in ammonia. At higher metal-atom concentrations, the material develops a bronze color, indicating that an insulator-metal transition has taken place. In many cases of interest, a continuum theoretical treatment is inconsistent because dimensions comparable with the average interatomic spacing are relevant.

In the last half-dozen years, the treatment of the topic in this review has undergone a revolution and a rebirth. The interactions of interest are of moderate range, the fluid atoms behave essentially classically, and the electron, though it must be treated quantum mechanically, responds to the slowly varying atomic positions; thus the system can be considered to consist of a few hundred atoms and an electron and is amenable to computer simulation. Various theoretical bases for such simulations have been developed. The most-developed methods are based on Feynman's path-integral approach to quantum statistical mechanics (Feynman and Hibbs, 1965). For the present applications, the approach was suggested by Chandler and Wolynes (1981; see also Chandler, 1984). Chandler *et al.* (1984) applied the method to an electron interacting with a hard-sphere fluid, and numerical results were given by Nichols *et al.* (1984). This approach focuses on the canonical partition function ($Z$) of the system composed of one electron and $N$ solvent atoms, where the electron-solvent interaction ($U_{es}$) is taken to be a superposition of hard-sphere potentials and the solvent-solvent interaction is $U_{ss}$. Within the adiabatic approximation, $Z$ can be written as the integral of a path-dependent action over all paths in imaginary time, using $\beta=1/kT$:

$$Z(\beta)=\int d\mathbf{R}_1\cdots\int d\mathbf{R}_N\int_{\text{path}} D[\mathbf{r}(t)] \times\exp[-W(\mathbf{r}(t),\{\mathbf{R}_i\})]\ , \tag{22}$$

$$W(\mathbf{r}(t),\{\mathbf{R}_j\})=\frac{1}{\hbar}\int_0^{\beta\hbar}dt\left[\frac{m|\dot{\mathbf{r}}|^2}{2}+U_{es}(r(t),\{\mathbf{R}_j\})\right] +\beta U_{ss}(\{\mathbf{R}_j\})\ , \tag{23}$$

and $D[\mathbf{r}(t)]$ is the differential element of path. The path is periodic in the interval $0\le t\le\beta\hbar$. The path integral is then discretized into $P$ equally spaced time steps, and the path between time steps is approximated by a straight line. In the limit of an infinite number of steps, the formulation becomes exact:

$$Z(\beta)=\int d\mathbf{R}_1\cdots\int d\mathbf{R}_N\exp[-\beta U_{ss}(\{\mathbf{R}_j\})] \times\int\prod_{\alpha=1}^{P}d\mathbf{r}^{(\alpha)}\{(2\pi\lambda_e^2/P)^{-3/2}\exp[-\beta u(|\mathbf{r}^{(\alpha)}-\mathbf{r}^{(\alpha+1)}|)\}\exp[-\beta U_{es}(\mathbf{r}^{(\alpha)},\{\mathbf{R}_j\})/\mathbf{P}]\ ; \tag{24}$$

the term in curly brackets in (24) is the free-electron density matrix, with the square of the electron de Broglie wavelength being $\lambda_e^2=\beta\hbar^2/m$, and $u(x)=(P/\beta\lambda_e^2)x^2/2$. The approximation becomes adequate (convergent) for a finite number of steps, and the path periodicity is maintained with $\mathbf{r}^{(1)}=\mathbf{r}^{(P+1)}$. The crux of the method is that the above problem is isomorphic to that of a classical, flexible ring polymer interacting with the solvent. The number of particles within the ring is equal to the number of time steps ($P$), and there are only harmonic nearest-neighbor interactions [$u(x)$, with a spring constant $P/\beta\lambda_e^2$] among the particles making up the ring polymer. Such a classical problem can be solved numerically or in some suitable approximation. Due to interaction with the solvent, the electron (ring polymer) may be forced to localize (i.e., self-trap). Results from this type of approach will be discussed later in this section. An alternative in this method is to use molecular dynamics to evaluate path integrals; this alternative was followed by Parrinello and Rahman (1984) to explore the localization of an excess electron in molten KCl. Various path-integral simulation methods were reviewed by Berne and Thirumalai (1986), along with applications that had been carried out.

Molecular dynamics have also been implemented using a quantal time-dependent self-consistent-field approach (see a review of methods by Kosloff, 1988). This approach uses the adiabatic Born-Oppenheimer approximation to decompose the problem into the atomic motion, responding to their mutual interaction and a mean in-

teraction due to the electron, and into the electronic motion, developing in response to the time-dependent Schrödinger equation with the instantaneous nuclear positions as parameters. In the most common approach, the electron wave function is described in momentum space and time propagated (discrete time steps); then it is Fourier transformed (fast-Fourier-transform numerical algorithms) to coordinate space, since it is needed in this form to calculate the effective interaction on the nuclei. This approach is usually limited to electronic ground-state occupancy, but may be extended to calculation of electronic excited states, with the nuclei in equilibrium with the electronic ground state, in order to calculate, for example, optical-absorption spectra (see the review of the hydrated electron problem, including optical-absorption spectra, by Rossky and Schnitker, 1988). Details will be discussed later. Cluster calculations have been recently reviewed (Jortner *et al.*, 1989).

An explosion of results has appeared in the literature and representative ones are quoted below. The problems treated encompass an electron in fluid helium (Bartholomew *et al.*, 1985; Kalia *et al.*, 1989, 1990), an electron in helium and comparison with one in xenon (Coker *et al.*, 1987; also see Laria and Chandler, 1987), in a statically disordered material (Sprik *et al.*, 1985a, 1985b, 1985c), in polar liquids (Barnett *et al.*, 1989), in molten salts (Parrinello and Rahman, 1984), and in finite clusters (see references in Posey *et al.*, 1989). Once the system has been equilibrated, the simulations can determine if the electron becomes localized in dimensions small compared to that of the system; the diffusion properties can be determined (Selloni *et al.*, 1987); electron excited states can be found for nuclear configurations in equilibrium with the electronic ground state; and optical-absorption spectra can be calculated (Schnitker *et al.*, 1988; Rajagopal *et al.*, 1990). In the case of finite clusters, electron localization has been observed both within the cluster and exterior to it (Barnett *et al.*, 1987). Generally, the simulations yield results in good agreement with experimental observations. The general features arising from previous discussion in this review are confirmed in the simulations. The basic problem of simulations is that results can only be obtained for the specific system under simulation, rather than with some generality.

Calculations, applying these new techniques, for systems in which an electron interacts with a hard-sphere or Lennard-Jones fluid, and for those in which it interacts with a static disordered medium, are directly comparable with the previously discussed work. The path-integral approach was first implemented directly, without use of simulation techniques but in a mean-field model, to investigate an electron interacting with a hard-sphere fluid via a hard-sphere potential (Chandler *et al.*, 1984 and numerical results by Nichols *et al.*, 1984). These authors obtained results that confirm that, at sufficiently high fluid density, electron self-trapping takes place in cavities. As the temperature is increased, the fluid density required to yield self-trapping also increases. The cavities are essentially spherical, and at high fluid densities there is total exclusion of atoms from the localization region. The calculations consider thermal equilibrium and deduce that only the electron ground state is of importance at high fluid densities—a result labeled as "ground-state dominance." All these results are in qualitative agreement with those previously discussed for an electron in helium.

As an example of the methods and results obtained with the above techniques, those of Nichols *et al.* (1984) are sketched in what follows. The system is an electron and a set of solvent atoms. The solvent-solvent interactions are of the hard-sphere type with sphere diameter $\sigma$; the electron-solvent interaction is also a hard-sphere one with a distance of closest approach $d$. Localization of the electron may be probed by examining the second moment of the ring correlation function:

$$R^2(t-t')=\langle |\mathbf{r}(t)-\mathbf{r}(t')|^2 \rangle \ , \tag{25}$$

with $0 \le t-t' \le \beta\hbar$. The characteristic size of the polymer is $R(\beta\hbar/2)$. For a free particle,

$$R^2_{\text{free}}(\Delta t)=3\lambda_e^2 \Delta t(\beta\hbar-\Delta t)/(\beta\hbar)^2, \quad \lambda_e^2=\beta\hbar^2/m \ . \tag{26}$$

Thus $R_{\text{free}}(\beta\hbar/2)=0.87\lambda_e$, which is usually large compared to $\sigma$. For a localized electron, i.e., at high solvent density, the correlation length $R(\Delta t)$, becomes independent of $\Delta t$ (ground-state dominance), except for $|\Delta t| \le \hbar/\Delta E$, where $\Delta E$ is the lowest excitation energy of the electron, and the correlation length becomes comparable to the localization region. Figure 9 shows results obtained by these authors for the correlation length, as a function of the solvent density for two temperatures. Note the relatively sharp localization threshold between $0.10<\rho\sigma^3<0.15$, for $\lambda_e=16\sigma$, and the rather broad threshold between $0.3<\rho\sigma^3<0.5$, for $\lambda_e=6\sigma$ (for helium, for example, $\sigma=2.57$ Å). This is a characteristic result: a sharp threshold for low temperatures and a broad one for high temperatures. The lack of delocalization at high temperature and high density constitutes a discrepancy between these results and those of the older continuum model.

Monte Carlo techniques to evaluate path integrals (PIMC) were then used for the problem with an electron-atom hard-sphere interaction and two treatments for the atomic system: a disordered static medium and a hard-sphere fluid (Sprik, Klein, and Chandler, 1985a, 1985b, 1985c). The results at $\lambda_e=6\sigma$, $\rho\sigma^3=0.2$, are essentially the same for the hard-sphere fluid or the static disordered system. In the case of the static disordered medium, this work confirms that at low temperature, when occupation of the low-energy states is more pronounced, the electron dominantly resides in low-density regions of the material—the so-called Lifshitz traps, as was previously discussed in reference to Luttinger's work (1976a, 1976b), though the authors con-

clude that Luttinger's approximations underestimate the solvent density required for a given localization (judging from the free energy at a given density and temperature). For the fluid case, the authors obtained results indicating that the approximations of Nichols *et al.* overestimate the density required for a given localization (the results of this work for $\rho\sigma^3=0.2$ are the same as those of the previous one for $\rho\sigma^3=0.39$).

A more realistic model calculation for an electron in helium, using a pseudopotential electron-atom interaction and a Lennard-Jones interaction among helium atoms, was carried out for a temperature of 77 K by Bartholomew, Hall, and Berne (1985). They considered helium densities between 0.1 and 2 ($\times 10^{22}$ cm$^{-3}$) and obtained results reflecting localization in smaller regions for higher fluid densities. There are quantitative but not qualitative differences between the results in this work and those of Chandler *et al.* (1984) and Sprik *et al.* (1985a, 1985b, 1985c), partly reflecting a difference in temperature ($T\sim 400$ K in the previous work) and the details of the interactions. Bartholomew *et al.* obtain localization (about 80 percent of the time) followed by delocalization at $1.2\times 10^{22}$ cm$^{-3}$, though such results may depend on the approximation. Other results at 77 K are quoted below. In comparing with experimental electron mobilities (Bartels, 1975), the authors note that the experiments appear to suggest either more effective localization beginning at lower densities or explicitly dynamical effects.

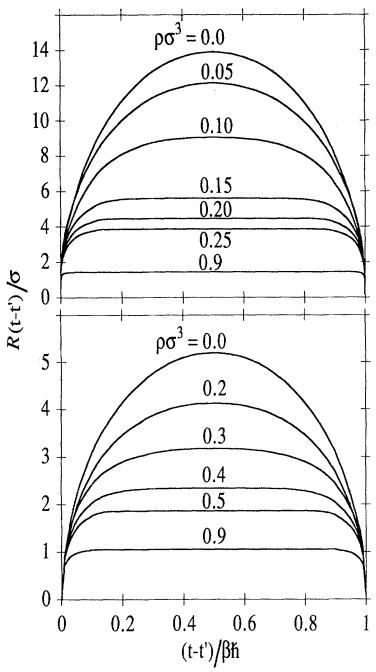


FIG. 9. Correlation length $R(t-t')$ [Eq. (25)], for $d=\sigma/2$, as a function of host density for two temperatures: $\lambda_e=16\sigma$ (upper curves) and $\lambda_e=6\sigma$ (lower curves); if $\sigma=5$ Å, the upper curves would correspond to 14 K and the lower ones to 100 K. A time-independent region at intermediate times is characteristic of localization with ground-state dominance (Nichols *et al.*, 1984).

It has been noted that polarization effects should be considered in letting an electron interact with a fluid. A first step in considering this problem in the path-integral context was taken by Nichols and Chandler (1986), who imbedded Drude oscillators in their hard spheres to allow an electron a further interaction. In broad lines, this work indicated that self-trapping was dominated by the excluded volume interactions, though the polarization effects did affect the solvation energy. Given possible technical deficiencies in the previous electron-helium calculations and the desire to explore the effects of polarization, Coker, Berne, and Thirumalai (1987) undertook PIMC calculations of an electron in helium (309 K) and in xenon (309 and 248 K), with realistic electron-atom pseudopotentials and Lennard-Jones fluids. Comparison with the hard-sphere calculations of Sprik *et al* (1985a, 1985b, 1985c) may be aided by the structural differences that have been noted between hard-sphere and Lennard-Jones fluids (see Laria and Chandler, 1987). The results of Coker *et al.* for electrons in helium (309 K) suggest that beyond a helium density of $1.8\times 10^{22}$ cm$^{-3}$ the cavity is well defined and there is ground-state dominance. This is not the case for a density of $0.6\times 10^{22}$ cm$^{-3}$. These results should be compared with the predictions of the old continuum model (Hernandez, 1975a) of metastable self-trapping, at this temperature, for a density of $1.2\times 10^{22}$ cm$^{-3}$ and stable self-trapping (by $\sim 2kT$ relative to the free state) by $1.6\times 10^{22}$ cm$^{-3}$. Parenthetically, calculations by Kalia *et al.* (1990), to be briefly discussed below, show metastable localization for the electron in helium at 77 K, beginning at $0.6\times 10^{22}$ cm$^{-3}$, which is also in excellent agreement with the older model referred to above (see Fig. 4). The xenon work of Coker *et al.* indicates that the polarization part of the electron-atom interaction strongly influences the electron, in contrast to the case in helium. This attractive interaction causes substantial enhancement of the atomic density in the environments of the electron (substantial enhancements of the electron-atom correlation function at distances beyond the short-range repulsion distance) and appears to lead to localization at subcritical temperatures (in the metastable two-phase regime for bulk xenon), but not at very low or very high densities; such behavior was previously discussed and had been very crudely estimated (Hernandez, 1983). Coker *et al.* also obtained an enhanced atomic density in the environment of the electron, in the regime where the bulk fluid has a stable single phase, but do not observe obvious localization. The experimental results (Huang and Freeman, 1978) are also ambiguous.

Finally, quantum molecular dynamics in the adiabatic Born-Oppenheimer approximation have been carried out for an electron in helium at 77 K (Kalia *et al.*, 1989, 1990). The latter work may be used as an example of the

method and results. These authors use an electron-helium interaction $v$ described by the pseudopotential of Kestner *et al.* (1965); the helium-helium interactions $U$ are of the Lennard-Jones type ($\varepsilon=10.22$ K, $\sigma=2.576$ Å). The electron obeys the time-dependent Schrödinger equation; thus the time development of the wave function may be written as

$$\psi(\mathbf{r},t+\Delta t)=\exp(i\Delta t\nabla^2/4m)\exp\left[-i\Delta t\sum_i v(\mathbf{r}-\mathbf{R}_j)\right]\times\exp(i\Delta t\nabla^2/4m)\psi(\mathbf{r},t)+O[(\Delta t)^3]\ . \quad (27)$$

The atoms are treated classically and therefore obey

$$M\ddot{\mathbf{R}}_j=-\nabla_j U(\{\mathbf{R}_i\})-\nabla_j\int d\mathbf{r}|\psi(\mathbf{r},t)|^2 v(\mathbf{r}-\mathbf{R}_j)\ . \quad (28)$$

Implementation of Eq. (27) has three steps, two of which use fast-Fourier-transform (FFT) techniques. First, carry out the FFT to take $\psi(\mathbf{r},t)\rightarrow\psi(\mathbf{k},t)$, which is time propagated and then inverse FFT:

$$e^{i\Delta t\nabla^2/4m}\psi(\mathbf{r},t)=\sum_k \psi(\mathbf{k},t)e^{-i\Delta t k^2/2m}e^{i\mathbf{k}\cdot\mathbf{r}}\ . \quad (29)$$

Then, multiply by the middle exponential in (27). Finally, repeat FFT, time propagation, and inverse FFT. The classical equation (28) is numerically integrated using various algorithms. Carrying out these procedures in a periodic box, for densities of $n=\rho\sigma^3=0.1$, 0.17, and 0.25 (i.e., $\rho=0.61$, 1.0, and $1.46\times10^{22}$ cm$^{-3}$, with 512 atoms for the lower densities and either 64 or 140 atoms for the highest density), they obtained results that may be quoted in terms of the participation ratios:

$$p(t)=\left[\Omega\int d\mathbf{r}|\psi(\mathbf{r},t)|^4\right]^{-1}, \quad (30)$$

normalized to the volume of the $n=0.1$ molecular-dynamics box. A large value of this function corresponds to a delocalized particle, a small value to localization. For $n=0.17$, $p(t)$ is essentially constant at $\sim10^{-2}$—corresponding to a localized particle. Calculation of the electron-helium radial distribution function $G(r)$, relative to the electron center of mass, yields the results of Fig. 10. It is clear that the electron occupies an essentially empty cavity of radius $\sim12$ a.u. (atomic units). Such excluded volume is also present for $n=0.25$. However, for $n=0.1$, the $p(t)$ obtained is shown in Fig. 11. It can be seen that for this case the simulation was begun with a localized electron; but it delocalized (3 ps), relocalized (4 ps), delocalized again (8 ps, to a dimension probably limited by the simulation cell), and then relocalized (10 ps). This process was expected to continue. Therefore, for such a helium density, it appears that localization is barely stable or metastable; the electron then samples localized and delocalized states as a function of time. It appears that the electron localizes to form a bubble for densities above $0.6\times10^{22}$ cm$^{-3}$ (as noted above); the bubbles are nearly spherical and, at higher helium densities, have excited states to which optical absorption is calculated by these authors. Such results are in good agreement with experiment and with older predictions with much more simplified assumptions and continuum models, which were previously reviewed.

In summary, path-integral and molecular-dynamics calculations for an electron in a fluid can yield results of high precision. The calculations are able to describe the extent of electron localization in thermal equilibrium and correlation functions between the electron and the fluid atoms. Optical spectra and electron mobilities are also accessible to this work. The results that have been obtained confirm the physical description previously given, which arose from simple continuum models. The onset of localization in helium, as a function of temperature, seems well described by the results quoted in Fig. 4.

There is insufficient space in this article to do justice to

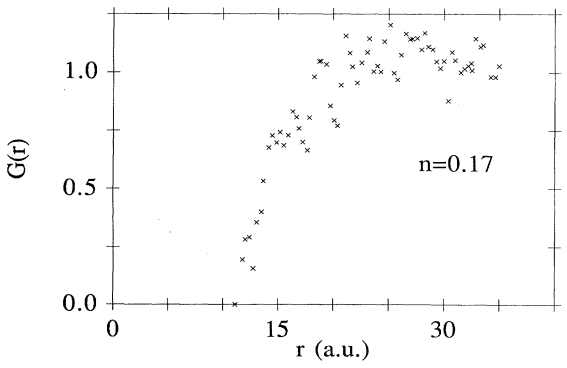


FIG. 10. Electron-helium radial distribution function $G(r)$ measured relative to the localized electron center of mass, for a helium density $n=0.17$ (i.e., $10^{22}$ cm$^{-3}$) and 77 K (Kalia *et al.*, 1990).

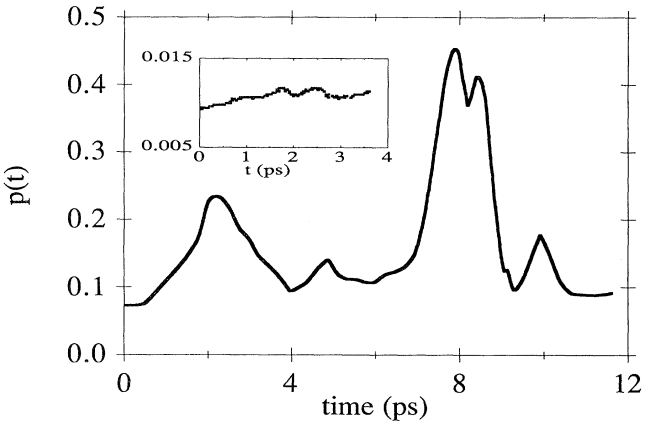


FIG. 11. Electron participation ratio $p(t)$ [see Eq. (30)] vs time in picoseconds, for a helium density $n=0.1$ (i.e., $6\times10^{21}$ cm$^{-3}$) ($n=0.17$ in inset) and 77 K. A small $p(t)$ denotes electron localization. Note the changes between localization and delocalization for the lower helium density. The calculated points have been smoothed to a continuous line (Kalia *et al.*, 1990).

all such recent topics. Therefore suffice it to note that the concepts established in the previous sections have a natural application to more complicated materials. Moreover, these concepts and associated phenomena must also be considered in discussing radiation chemistry, the rates of chemical reactions involving electrons in fluids, and even insulator-metal transitions in fluids.

## IX. OVERVIEW

For the fluids of simple atomic systems, one can summarize the available states for electrons as follows. The high-kinetic-energy states are delocalized and the density of states is free-electron-like; the potential fluctuations are irrelevant to the density of states, compared to the kinetic energy. At low electron energy, in these systems, the states are localized in space. The density of states decreases with decreasing energy, and such states are due to inhomogeneities in the material that yield regions that are more attractive than average to the electron. For low electron energy, the region must not only be attractive (low potential), it must also be large (low electron kinetic energy). Thus, as the electron energy is decreased, the suitable regions in the material become increasingly improbable—decreasing the available density of states. While the energy scale is determined by the average potential ($E_0$), this does not mean that all states above $E_0$ are delocalized. Due to the potential fluctuations, the relative potential-to-kinetic-energy scale plays a role in determining where the localization threshold, also called the mobility edge, is with respect to $E_0$. In thermal equilibrium, the electrons in the system occupy the states with a Fermi distribution appropriate to the system temperature and the electron concentration (which fixes the chemical potential). For low electron densities and low temperatures, the energy range with non-negligible occupation probability may be relatively narrow. In such a case, all occupied configurations may be similar, and it is adequate to describe them as a single state (particle in a well of fixed radius, for example). In the case in which the total density of localized states is small (a low fluid density, for example) and the temperature high, the most probable occupied state may be delocalized, but some fraction of the electrons must be in the (low electron energy) localized states. In the transition between these regimes the density of electron states is smoothly varying.

The localized electron states in fluid He and Ne (and in $H_2$ and $N_2$) are associated with regions of lower density than average, due to the dominant short-range repulsion of an electron and an atom. On average, polarization effects are minor in comparison with the Pauli repulsion, even though the polarization interaction is long-ranged. The situation reverses for the highly polarizable heavy rare gases Xe and Kr; in these cases the fluids have a higher density than average near the electron, although the Pauli repulsion may lead to short-range density oscillations. In fluid argon the situation is very unclear; the theory must contend with both the short-range repulsion and the longer-ranged screened polarization without a clear dominance.

In more complicated nonpolar materials (methane and ethane, for example), the general features are as previously described, but with additional complications due to intermolecular interactions and steric constants. For polar materials (as are ammonia and water) the situation is further complicated by the permanent dipole moments and hydrogen bonding. Localization in regions of a size comparable to the intermolecular separations takes place in this last class of materials and thus precludes a continuum model, at least in the immediate neighborhood of the localization center.

In this article a discussion of the basic physics and some phenomena concerning self-trapping of electrons and other light particles in simple fluids has been presented. Without deviating too far from this central topic, some applications and related effects have been described. It is hoped that the nonspecialist reader has developed an appetite for looking further into this field and that some specialists have been given a point of view that will spur them to unravel fascinating phenomena that exist in this area.

## REFERENCES


Anderson, P. W., 1958, Phys. Rev. B **109**, 1492.

Andrei, E. Y., 1984, Phys. Rev. Lett. **52**, 1449.

Ashcroft, N. W., and N. D. Mermin, 1976, *Solid State Physics* (Saunders, Philadelphia).

Atkins, K. R., 1959, Phys. Rev. **116**, 1339.

Bachelet, G. B., D. R. Hamann, and M. Schlüter, 1982, Phys. Rev. B **26**, 4199.

Barenghi, C. F., G. J. Mellor, C. M. Muirhead, and W. F. Vinen, 1986, J. Phys. C **19**, 1135.

Barnett, R. N., U. Landman, C. L. Cleveland, and J. Jortner, 1987, Phys. Rev. Lett. **59**, 811.

Barnett, R. N., U. Landman, and A. Nitzan, 1989, Phys. Rev. Lett. **62**, 106.

Bartels, A., 1973, Phys. Lett. A **45**, 491.

Bartels, A., 1975, Appl. Phys. **8**, 59.

Bartholomew, J., R. W. Hall, and B. J. Berne, 1985, Phys. Rev. B **32**, 548.

Basak, S., and M. H. Cohen, 1979, Phys. Rev. B **20**, 3404.

Baym, G., R. G. Barrera, and C. J. Pethik, 1969, Phys. Rev. Lett. **22**, 20.

Berger, H. R., and J. P. Hernandez, 1982, Phys. Rev. B **26**, 2733.

Berne, B. J., and D. Thirumalai, 1986, in *Annual Review of Physical Chemistry 37*, edited by H. H. Strauss, G. L. Babcock, and C. Bradley-Moore (Annual Reviews, Palo Alto), p. 401.

Borghesani, A. F., L. Bruschi, M. Santini, and G. Torzo, 1988, Phys. Rev. A **37**, 4828.

Borghesani, A. F., and M. Santini, 1990a, presentation at the Sixth International Symposium on Gaseous Dielectrics, Sept. 23–27, Knoxville, TN (unpublished).

Borghesani, A. F., and M. Santini, 1990b, Phys. Rev. A **42**, 7377.

Born, M., and J. R. Oppenheimer, 1927, Ann. Phys. (NY) **84**, 457.

Braglia, G. L., and V. Dallacassa, 1982, Phys. Rev. A **26**, 902.
Briscoe, C. V., S.-I. Choi, and A. T. Stewart, 1968, Phys. Rev. Lett. **20**, 493.
Brown, T. R., and C. C. Grimes, 1972, Phys. Rev. Lett. **29**, 1233.
Bruschi, L., B. Maraviglia, and F. Moss, 1966, Phys. Rev. Lett. **17**, 682.
Bruschi, L., G. Mazzi, and M. Santini, 1972, Phys. Rev. Lett. **28**, 1504.
Bruschi, L., G. Mazzi, M. Santini, and G. Torzo, 1975, J. Phys. C **8**, 1412.
Bruschi, L., M. Santini, and G. Torzo, 1984a, J. Phys. B **17**, 1137.
Bruschi, L., M. Santini, and G. Torzo, 1984b, Phys. Lett. A **102**, 102.
Canter, K. F., J. D. McNutt, and L. O. Roellig, 1975, Phys. Rev. A **12**, 375.
Careri, G., U. Fasoli, and F. S. Gaeta, 1960, Nuovo Cimento **15**, 774.
Careri, G., F. Scaramuzzi, and J. O. Thompson, 1959, Nuovo Cimento **13**, 186.
Chandler, D., 1984, J. Phys. Chem. **88**, 3400.
Chandler, D., Y. Singh, and D. M. Richardson, 1984, J. Chem. Phys. **81**, 1975.
Chandler, D., and P. G. Wolynes, 1981, J. Chem. Phys. **74**, 4078.
Cleveland, C. L., and H. A. Gersch, 1981, Phys. Rev. A **23**, 261.
Coker, D. F., B. J. Berne, and D. Thirumalai, 1987, J. Chem. Phys. **86**, 5689.
Cole, M. W., 1970, Phys. Rev. B **2**, 4239.
Cole, M. W., and M. H. Cohen, 1969, Phys. Rev. Lett. **23**, 1238.
Cole, M. W., and J. R. Klein, 1979, J. Low Temp. Phys. **36**, 331.
Crandal, R. S., and R. Williams, 1971, Phys. Lett. A **34**, 404.
Dahm, A. J., and W. F. Vinen, 1987, Phys. Today **40**, No. 2, 43.
Daniel, T. B., and R. Stump, 1959, Phys. Rev. **115**, 1599.
Degani, M. G., and O. Hipolito, 1985, Phys. Rev. B **32**, 3300.
Deville, G., A. Valder, E. Y. Andrei, and F. I. B. Williams, 1984, Phys. Rev. Lett. **53**, 588.
Duff, B. G., and F. F. Heyman, 1962, Proc. R. Soc. London A **270**, 517.
Ebner, C., and C. Punyanitya, 1979, Phys. Rev. A **19**, 856.
Eggarter, T. P., 1972, Phys. Rev. A **5**, 2496.
Eggarter, T. P., and M. H. Cohen, 1970, Phys. Rev. Lett. **25**, 807.
Eggarter, T. P., and M. H. Cohen, 1971, Phys. Rev. Lett. **27**, 129.
Ellis, T., P. V. E. McClintock, and R. M. Bowley, 1983, J. Phys. C **16**, L485.
Farazdel, A., 1986, Phys. Rev. Lett. **57**, 2664.
Ferrell, R. A., 1958, Phys. Rev. **108**, 167.
Fetter, A., 1975, in *The Physics of Liquid and Solid Helium,* Part I, edited by K. H. Bennemann and J. B. Ketterson (Wiley, New York), p. 207.
Feynman, R. P., and A. R. Hibbs, 1965, *Quantum Mechanics and Path Integrals* (McGraw-Hill, New York).
Fisher, D. S., B. J. Halperin, and P. M. Platzman, 1979, Phys. Rev. Lett. **42**, 798.
Fowler, W. B., and D. L. Dexter, 1968, Phys. Rev. **176**, 337.
Glaberson, W. I., and K. W. Schwarz, 1987, Phys. Today **40**, No. 2, 54.
Glattili, D. C., E. Y. Andrei, G. Deville, J. Pointrenaud, and F. I. B. Williams, 1985, Phys. Rev. Lett. **54**, 1710.
Grimes, C. C., 1978, Surf. Sci. **73**, 379.
Grimes, C. C., 1991, private communication.
Grimes, C. C., and G. Adams, 1976, Phys. Rev. Lett. **36**, 145.
Grimes, C. C., and G. Adams, 1979, Phys. Rev. Lett. **42**, 795.
Grimes, C. C., and G. Adams, 1990, Phys. Rev. B **41**, 6366.
Harrison, H. R., and B. E. Springett, 1971a, Phys. Lett. A **35**, 73.
Harrison, H. R., and B. E. Springett, 1971b, Chem. Phys. Lett. **10**, 418.
Hernandez, J. P., 1973, Phys. Rev. A **7**, 1755.
Hernandez, J. P., 1975a, Phys. Rev. B **11**, 1289.
Hernandez, J. P., 1975b, Phys. Rev. B **12**, 3975.
Hernandez, J. P., 1976, Phys. Rev. A **14**, 1579.
Hernandez, J. P., 1977, Phys. Rev. B **15**, 5078.
Hernandez, J. P., 1983, J. Phys. C **16**, 3465.
Hernandez, J. P., H. R. Berger, and D. W. Smith, 1979, Phys. Rev. B **20**, 5330.
Hernandez, J. P., and S.-I. Choi, 1969, Phys. Rev. **188**, 340.
Hernandez, J. P., and L. W. Martin, 1991a, Phys. Rev. A **43**, 4568.
Hernandez, J. P., and L. W. Martin, 1991b, submitted for publication.
Hirschfelder, J. O., C. F. Curtiss, and R. B. Bird, 1954, *Molecular Theory of Gases and Liquids* (Wiley, New York), p. 339.
Holroyd, R. A., 1987, in *Radiation Chemistry: Principles and Applications,* edited by Farhataziz and M. A. J. Rodgers (VCH, New York), p. 201.
Huang, Sam S.-S., and G. R. Freeman, 1978, J. Chem. Phys. **68**, 1355.
Huang, Sam S.-S., and G. R. Freeman, 1981, Phys. Rev. A **24**, 714.
Iakubov, I. T., and A. G. Khrapak, 1982, Rep. Prog. Phys. **45**, 697.
Jahnke, J. A., L. Meyer, and S. Rice, 1971, Phys. Rev. A **3**, 734.
Jahnke, J. A., M. Silver, and J. P. Hernandez, 1975, Phys. Rev. B **12**, 3420.
Jortner, J., N. R. Kestner, S. A. Rice, and M. H. Cohen, 1965, J. Chem. Phys. **43**, 2614.
Jortner, J., D. Sharf, and U. Landman, 1989, in *Elemental and Molecular Clusters,* edited by G. Benedek, T. P. Martin, and G. Pacchioni (Springer, Berlin), p. 148.
Kajita, K., and W. Sasaki, 1982, Surf. Sci. **113**, 419.
Kalia, R. K., P. Vashishtra, and S. W. de Leeuw, 1989, J. Chem. Phys. **90**, 6802.
Kalia, R. K., P. Vashishta, S. W. de Leeuw, and J. Harris, 1990, in *Strongly Coupled Plasma Physics,* edited by S. Ichimaru (Elsevier/Yamada Science Foundation, Japan), p. 93.
Kestner, N. R., 1976, in *Electron-Solvent and Anion-Solvent Interactions,* edited by L. Kevan and B. C. Webster (Elsevier, Amsterdam), p. 1.
Kestner, N. R., J. Jortner, M. H. Cohen, and S. A. Rice, 1965, Phys. Rev. **140**, A56.
Kosloff, R., 1988, J. Phys. Chem. **92**, 2087.
Kosterlitz, J. M., B. J. Thouless, 1973, J. Phys. C **6**, 1191.
Kuper, C. G., 1961, Phys. Rev. **122**, 1007.
Landau, L. D., 1933, Phys. Z. Sowjetunion **3**, 664.
Laria, D., and D. Chandler, 1987, J. Chem. Phys. **87**, 4088.
LeComber, P. G., J. B. Wilson, and R. J. Loveland, 1976, Solid State Commun. **18**, 377.
Leiderer, P., W. Ebner, and V. B. Shikin, 1982, Surf. Sci. **113**, 405.
Lekner, J., 1967, Phys. Rev. **158**, 130.
Lekner, J., 1968a, Philos. Mag. **18**, 1281.
Lekner, J., 1968b, Phys. Lett. A **27**, 341.
Levine, J. L., and T. M. Sanders, Jr., 1962, Phys. Rev. Lett. **8**, 159.

Levine, J. L., and T. M. Sanders, Jr., 1967, Phys. Rev. **154**, 138.
Loveland, R. J., P. G. LeComber, and W. E. Spear, 1972, Phys. Lett. A **39**, 225.
Luttinger, J. M., 1976a, Phys. Rev. Lett. **37**, 609.
Luttinger, J. M., 1976b, Phys. Rev. B **13**, 2596.
Martin, L. W., 1991, Ph.D. thesis (University of North Carolina at Chapel Hill).
Mast, D. B., A. J. Dahm, and A. L. Fetter, 1985, Phys. Rev. Lett. **54**, 1706.
Meyer, L., and F. Reif, 1958, Phys. Rev. **110**, 279.
Miller, B. N., and T. Reese, 1989, Phys. Rev. A **39**, 4735.
Miyakawa, T., and D. L. Dexter, 1970, Phys. Rev. A **1**, 513.
Moore, R. L., C. L. Cleveland, and H. A. Gersch, 1978, Phys. Rev. B **18**, 1183.
Nakanishi, H., and D. M. Schrader, 1986a, Phys. Rev. A **34**, 1810.
Nakanishi, H., and D. M. Schrader, 1986b, Phys. Rev. A **34**, 1823.
Nelson, D. R., and B. I. Halperin, 1979, Phys. Rev. B **19**, 2457.
Nichols, A. L., and D. Chandler, 1986, J. Chem. Phys. **84**, 398.
Nichols, A. L., D. Chandler, Y. Singh, and D. M. Richardson, 1984, J. Chem. Phys. **81**, 5109.
Nieminen, R. M., M. Manninen, I. Väliman, and P. Hautojärvi, 1980, Phys. Rev. A **21**, 1677.
Northby, A., and T. M. Sanders, Jr., 1967, Phys. Rev. Lett. **18**, 1184.
O'Malley, T. F., 1963, Phys. Rev. **130**, 1020.
O'Malley, T. F., 1980, J. Phys. B **13**, 1491.
Onn, D. G., and M. Silver, 1969, Phys. Rev. **183**, 295.
Onn, D. G., and M. Silver, 1971, Phys. Rev. A **3**, 1773.
Ostermeier, R. M., 1973, Phys. Rev. A **8**, 514.
Ott-Rowland, M. L., V. Kotsubo, J. Theobald, and G. A. Williams, 1982, Phys. Rev. Lett. **49**, 1708.
Paalanen, M. A., and Y. Iye, 1985, Phys. Rev. Lett. **55**, 176.
Padmore, T. C., and M. W. Cole, 1974, Phys. Rev. A **9**, 802.
Parks, P. E., and R. J. Donnelly, 1966, Phys. Rev. Lett. **16**, 45.
Parrinello, M., and A. Rahman, 1984, J. Chem. Phys. **80**, 860.
Paul, D. A. L., and R. L. Graham, 1957, Phys. Rev. **106**, 16.
Plenkiewicz, B., C. Plenkiewicz, C. Houée-Levin, and J.-P. Jay-Gerin, 1988, Phys. Rev. A **38**, 6120.
Plenkiewicz, B., C. Plenkiewicz, and J.-P. Jay-Gerin, 1988, Phys. Rev. A **38**, 4460.
Plenkiewicz, B., C. Plenkiewicz, and J.-P. Jay-Gerin, 1989, Phys. Rev. A **39**, 2070.
Pointrenaud, J., and F. I. B. Williams, 1972, Phys. Rev. Lett. **29**, 1230.
Posey, L. A., P. J. Campagnola, M. A. Johnson, G. H. Lee, J. G. Eaton, and K. H. Bowen, 1989, J. Chem. Phys. **91**, 6536.
Rajagopal, G., R. N. Barnett, A. Nitzan, U. Landman, E. C. Honea, P. Labastie, M. L. Homer, and R. L. Whetten, 1990, Phys. Rev. Lett. **64**, 2933.
Rayfield, G. S., and F. Reif, 1963, Phys. Rev. Lett. **11**, 305.
Roellig, L. O., and T. M. Kelly, 1967, Phys. Rev. Lett. **18**, 387.
Rossky, P. J., and J. Schnitker, 1988, J. Phys. Chem. **92**, 4277.
Schnitker, J., K. Motakabbir, P. J. Rossky, and R. Friesner, 1988, Phys. Rev. Lett. **60**, 4561.
Schoepe, W., and G. W. Rayfield, 1973, Phys. Rev. A **7**, 2111.
Schoepe, W., and F. Wagner, 1975, Phys. Rev. B **12**, 3973.
Schwarz, K. W., 1975, in *Advances in Chemical Physics,* Vol. XXXIII, edited by I. Prigogine and S. A. Rice (Wiley, New York), p. 1.
Schwarz, K. W., 1980, Phys. Rev. B **21**, 5125.
Selloni, A., P. Carnevali, R. Car, and M. Parrinello, 1987, Phys. Rev. Let. **59**, 823.
Shikin, V. B., 1970, Zh. Eksp. Teor. Fiz. **58**, 1948 [Sov. Phys. JETP **31**, 936 (1970)].
Shikin, V. B., 1971, Zh. Eksp. Theor. Fiz. **60**, 713 [Sov. Phys. JETP **33**, 387 (1971)].
Simon, S. H., V. Dobrosavljević, and R. M. Stratt, 1990, Phys. Rev. A **42**, 6278.
Smejtec, P., M. Silver, K. S. Dy, and D. G. Onn, 1973, J. Chem. Phys. **59**, 1374.
Smith, D. W., and J. P. Hernandez, 1982, J. Chem. Phys. **77**, 5802.
Sommer, W. T., and D. J. Tanner, 1971, Phys. Rev. Lett. **27**, 1345.
Sprik, M., M. L. Klein, and D. Chandler, 1985a, Phys. Rev. B **31**, 4234.
Sprik, M., M. L. Klein, and D. Chandler, 1985b, Phys. Rev. B **32**, 545.
Sprik, M., M. L. Klein, and D. Chandler, 1985c, J. Chem. Phys. **83**, 3042.
Springett, B. E., 1967, Phys. Rev. **155**, 139.
Springett, B. E., and R. J. Donnelly, 1966, Phys. Rev. Lett. **17**, 364.
Springett, B. E., J. Jortner, and M. H. Cohen, 1968, J. Chem. Phys. **48**, 2720.
Stott, M. J., and E. Zaremba, 1977, Phys. Rev. Lett. **38**, 1493.
Tauchert, W., H. Jungblut, and W. F. Schmidt, 1977, Can. J. Chem. **55**, 1860.
Tawel, R., and K. F. Canter, 1986, Phys. Rev. Lett. **56**, 2322.
Triftshäuser, W., J. Legg, A. T. Stewart, and C. V. Briscoe, 1968, in *Proceedings of the 11th International Conference on Low Temperature Physics, St. Andrews, Scotland, 1968,* Vol. 1, edited by J. F. Allen, D. M. Finlayson, and D. M. McCall (University of St Andrews, St. Andrews, Scotland), p. 304.
Tuomisaari, M., K. Rytsölä, and P. Hautojärvi, 1988, Phys. Lett. A **112**, 279.
von Zdrojewski, W., J. G. Rabe, and W. F. Schmidt, 1980, Z. Naturforsch. A **35**, 672.
Wackerle, J., and R. Stump, 1957, Phys. Rev. **106**, 18.
Weyl, W., 1863, Ann. Phys. (Leipzig) **197**, 601.
Williams, G. A., and R. E. Packard, 1974, Phys. Rev. Lett. **33**, 280.
Young, R. A., 1970, Phys. Rev. A **2**, 1983.
Zipfel, C., and T. M. Sanders, Jr., 1968, in *Proceedings of the 11th International Conference on Low Temperature Physics, St. Andrews, Scotland, 1968,* Vol. 1, edited by J. F. Allen, D. M. Finlayson, and D. M. McCall (University of St. Andrews, St. Andrews, Scotland), p. 296.